Critical Role for the Unique N-Terminus of Chlamydial MreB in Directing Its Membrane Association and Interaction with Elements of the Divisome

Junghoon Lee[1], John V. Cox[2], and Scot P. Ouellette[1]

[1] Department of Pathology and Microbiology, University of Nebraska Medical Center, Omaha, NE, USA 68198

[2] Department of Microbiology, Immunology, and Biochemistry, University of Tennessee Health Science Center, Memphis, TN, USA 38163

Abstract

Chlamydiae lack the conserved central coordinator protein of cell division FtsZ, a tubulin-like homolog. Current evidence indicates *Chlamydia* uses the actin-like homolog, MreB, to substitute for the role of FtsZ. Interestingly, we observed MreB as a ring at the septum in dividing cells of *Chlamydia*. We hypothesize that, for MreB to substitute for FtsZ in *Chlamydia*, it must possess unique properties compared to canonical MreB homologs. Sequence differences between chlamydial MreB and homologs in other bacteria revealed that chlamydial MreB possesses an extended N-terminal region as well as a conserved amphipathic helix found in other bacterial MreBs. The extended N-terminal region is sufficient to restore the localization of a truncated MreB mutant of *E.coli* lacking its amphipathic helix to the membrane and is crucial for interactions with cell division components RodZ and FtsK, though the region is not required for homotypic interactions. In addition, the N-terminal region was sufficient to direct GFP to the membrane when expressed in *Chlamydia*. From these data, the extended N-terminal region of chlamydial MreB is critical for correct localization and interactions of this protein. Our data provide mechanistic support for the ability of chlamydial MreB to serve as a substitute for FtsZ.

Word Count: 197/200

31 ## Importance

32 *Chlamydia* is an obligate intracellular bacterial pathogen, which causes sexually
33 transmitted diseases and trachoma. A better understanding of basic chlamydial physiology is
34 important for developing novel therapeutic strategies for these diseases. Chlamydiae divide by
35 a unique polarized cell division process not requiring the canonical cell division coordinator
36 FtsZ. We previously demonstrated a role for MreB in directing chlamydial division. We
37 hypothesize chlamydial MreB encodes unique features allowing it to substitute for FtsZ in this
38 organism. Here, we performed a detailed characterization of chlamydial MreB as a cell division
39 coordinator. Chlamydial MreB forms a ring at the septum, like FtsZ in *E.coli*. It possesses an
40 extended N-terminus that is conserved amongst *Chlamydiaeceae*. This region displays
41 amphipathicity that is sufficient to drive membrane localization of distinct proteins. In addition,
42 this region is crucial for interactions with other division proteins. We propose that this N-
43 terminal region confers unique properties to chlamydial MreB.

44 **Word count: 149/150**

45 ## Introduction

46 *Chlamydia* is an obligate intracellular pathogen that causes diverse diseases. These
47 Gram-negative cocci differentiate between two morphologically and functionally distinct
48 cellular forms during their developmental cycle: the elementary body (EB) and the reticulate
49 body (RB)(1). The EB is the infectious but non-dividing form whereas the RB is the dividing
50 but non-infectious form. After entering the host cell, *Chlamydia* remains within a membrane-
51 bound parasitic organelle, termed an inclusion(2). RBs undergo multiple rounds of cell division
52 until such point they engage a secondary differentiation program and convert to EBs, which
53 are subsequently released from the host cell to propagate the infection.

54 In evolving to obligate intracellular dependence, *Chlamydia* has significantly reduced
55 its genome and eliminated *ftsZ*(3), encoding the conserved tubulin-like cell division
56 coordinator of binary fission(4). However, *Chlamydia* encodes rod-shape determining proteins
57 associated with peptidoglycan synthesis in the lateral cell wall of bacilli. That *Chlamydia* has
58 retained these genes is unusual since these are coccoid bacteria and only synthesize
59 peptidoglycan during division(5). The absence of FtsZ in chlamydiae suggest they might not
60 divide by binary fission. Recent work from our labs supports this. We employed both live-cell
61 and fixed-cell imaging to localize various markers, including a cell division protein (FtsQ(6)),
62 during EB-to-RB differentiation and the first division of the RB. Interestingly, we observed
63 that chlamydiae are highly polarized throughout this time and that division itself occurs via a
64 polarized process(7). This polarized budding process remains the primary mode of division
65 even at later times during the developmental cycle (Cox et al., *in prep*).

66 In 2012, we hypothesized and presented evidence that *Chlamydia* co-opted the rod-
67 shape determining protein MreB to function as the central coordinator of division(8). To
68 perform this function, we hypothesize that chlamydial MreB possesses unique properties.

69 Many MreB homologs encode an N-terminal amphipathic helix that facilitates MreB
70 association with the inner membrane(9). At the membrane periphery it engages PG synthesis
71 along short moving filaments(10-12). Here, we investigated the unique structural features of
72 chlamydial MreB that allow it to substitute for FtsZ. Chlamydial MreB forms rings at the
73 division site, and bioinformatics analysis indicates that chlamydial MreB encodes an extended
74 N-terminal region (amino acids 1-23: aa1-23) in addition to the conserved amphipathic helix.
75 The aa1-23 residues also encode predicted amphipathicity. We confirmed that the conserved
76 amphipathic helix, but not aa1-23, is important for directing membrane-localization of GFP.
77 Nevertheless, when aa1-23 of chlamydial MreB was fused to a cytosolic *E. coli* MreB lacking
78 its endogenous amphipathic helix, *E. coli* MreB was redirected to the membrane. Importantly,
79 aa1-23 were sufficient to direct GFP to the membrane in *Chlamydia* directly. We determined
80 the unique N-terminal region of chlamydial MreB is crucial for its interactions with proteins
81 related to cell division but not its ability to form homo-oligomers. Our data indicate the unique
82 N-terminal region of chlamydial MreB is important for membrane localization and interaction
83 with the divisome. These properties may allow it to function as a central organizer of the cell
84 division machinery in *Chlamydia* and in a manner distinct from other MreB homologs.

85 ## Results

86 **Chlamydial MreB_6xH localizes as a ring at the division site.** Given our hypothesis for the
87 role of chlamydial MreB in directing polarized division, we examined its localization during
88 the first division of an RB. We were unable to detect endogenous MreB using the antibody
89 previously reported to image the distribution of MreB in *Chlamydia*(13). We then attempted to
90 image wild-type and various truncation mutants of MreB using a GFP sandwich (SW) fusion
91 strategy that, in *E. coli*, was reported to be functional(14) (N- or C-terminal fluorescent protein
92 fusions with MreB display an artifactual localization(15)). However, when we inducibly

93 expressed MreB_GFP$_{SW}$ in *C. trachomatis* L2, bacterial growth was significantly inhibited,
94 even with low levels of expression, as observed by the presence of a small number of enlarged
95 bacteria (Suppl. Fig. 1). We, therefore, opted to construct an MreB fusion with a small C-
96 terminal hexahistidine tag (MreB_6xH). The human epithelial cell line, HeLa, was infected
97 with a transformant of *C. trachomatis* L2 carrying a plasmid to inducibly express MreB_6xH.
98 At 6 hours post-infection (hpi), expression of MreB_6xH was induced with
99 anhydrotetracycline (aTc), and cells were fixed at 10.5 hpi, a time when the nascent RB has
100 begun its first division(7). As seen in Figure 1, we observed using super-resolution structured
101 illumination microscopy (SIM) the polar localization of the major outer membrane protein
102 (MOMP) in the budding daughter cell as previously reported(7). Consistent with its proposed
103 role in division(8), MreB_6xH was localized in a band-like structure across the septum and not
104 in puncta as previously reported(13, 16). Interestingly, when 3D reconstructions were
105 assembled from the SIM images, we observed that MreB_6xH formed clear ring-like structures
106 at the septum.

107 **Chlamydial MreB encodes an amphipathic helix and an extended N-terminal region**
108 **conserved in *Chlamydiae*.** In many Gram-negative bacteria, there is an amphipathic helix at
109 the N-terminus of MreB, and the helix is important for the membrane localization of MreB(9).
110 This localization is crucial for the role of MreB in directing PG synthesis during lateral cell
111 wall growth(9, 17). To confirm whether chlamydial MreB also has these features, we predicted
112 its secondary structure and amphipathic regions using bioinformatics tools (Fig. 2). The
113 alignment data show that chlamydial MreB encodes an extended N-terminal region (amino
114 acids 1-23: aa1-23), which other Gram-negative bacteria lack (Fig. 2A). Importantly, this
115 extended N-terminal region is conserved amongst *Chlamydiae* (Suppl. Fig. 2). Following this
116 region, there is a predicted amphipathic helix, from R24 to F29 (Fig. 2B), that aligns with the
117 amphipathic helices of the other bacteria (Fig. 2A). A high amphipathic score (A-score) extends

118 to residue F32 in chlamydial MreB. Interestingly, aa1-23 also has a high A-score though the
119 region was not predicted to form an amphipathic helix (Fig. 2B). Nevertheless, performing a
120 helical wheel analysis with 8 amino acid windows revealed that each window shows
121 amphipathicity (Fig. 2C). Based on these observations, we conclude that the extended N-
122 terminal region of chlamydial MreB may possess membrane-associating properties.

123 **Chlamydial MreB is unable to complement an *mreB*-deficient mutant of *E.coli.*** The
124 bioinformatics data suggested that chlamydial MreB encodes unique structural features absent
125 in other bacterial MreBs (Fig. 2A). To assess the activities associated with these unique
126 structural elements, we introduced chlamydial MreB into an *mreB*-deficient mutant of *E.coli.*
127 As *mreB* is an essential gene in *E.coli*, Bendezu et al. made the strain P2733, which has a
128 deletion in the *mreB* gene and is conditionally viable by the overexpression of the *ftsQAZ*
129 operon(18). This strain has been used for complementation assays and grows as coccoid
130 bacteria (since MreB is necessary for rod-shape)(18). To test whether chlamydial MreB
131 (CtrMreB) is capable of complementing the *mreB* deficient mutant, P2733 was transformed
132 with an arabinose-inducible vector encoding chlamydial *mreB*. Cell shape was compared after
133 inducing MreB expression in comparison to an empty vector negative control and an *E. coli*
134 MreB (EcMreB) positive control. When EcMreB is expressed from an arabinose-inducible
135 promoter in the P2733 strain, the *E. coli* cells begin to adopt a rod shape (Fig. 3B), consistent
136 with other reports(14, 18, 19). When chlamydial MreB was induced, the morphology of P2733
137 was unchanged compared to uninduced or empty vector controls, indicating that chlamydial
138 MreB does not complement the *mreB*-deficient mutant of *E.coli* (Fig. 3C). To determine
139 whether the inability of chlamydial MreB to complement was due to its extended N-terminal
140 region, we performed the same experiment with ΔN22 chlamydial MreB, which more closely
141 resembles *E. coli* MreB in size and characteristics at the N-terminus. We observed that ΔN22
142 chlamydial MreB also does not complement the *mreB* deficient *E.coli*, suggesting that the

143 extended N-terminal region is not the only reason for the failure to complement (Fig. 3D – see
144 also Discussion). Chlamydial MreB expression was confirmed in these experiments by western
145 blotting (Suppl. Fig. 3).

146 **The amphipathic helix, but not the extended N-terminal region, of chlamydial MreB is**
147 **sufficient to direct GFP to the membrane in *E. coli*.** We hypothesized that, because of their
148 amphipathicity, the unique sequence elements at the N-terminus of chlamydial MreB could
149 direct the membrane localization of MreB (Fig. 1). To test this, we performed a series of
150 localization studies in *E. coli* using the N-terminal regions of chlamydial MreB (CtrMreB)
151 fused to GFP. A similar strategy was used to demonstrate that two copies of the amphipathic
152 helix of *E. coli* MreB (EcMreB) were sufficient to direct GFP to the membrane(9). We made
153 various fusions in which portions of the N-terminal region of chlamydial MreB were fused to
154 GFP either in one copy or two (illustrated in Fig. 4A). We then observed the localization of
155 these proteins in both wild-type (MG1655) and MreB-deficient (P2733) *E.coli* (Fig. 4B and
156 Suppl. Fig. 4). We observed that a single copy of aa1-32 ($MreB_{1-32}$), encoding all high A-score
157 residues, was sufficient to direct GFP to the membrane. Interestingly, aa1-28 ($MreB_{1-28}$),
158 encoding both the predicted amphipathic helix and the extended N-terminus, was also sufficient
159 to direct GFP to the membrane, but, in wild-type cells, its localization was primarily restricted
160 to the poles. Consistent with *E. coli*, two copies of aa23-32 ($MreB_{23-32}$), encoding the predicted
161 amphipathic helix, directed GFP to the membrane. Contrary to our prediction, one or two copies
162 of aa1-23-GFP ($MreB_{1-23}$-GFP) was not able to direct GFP to the membrane even though the
163 region has a high A-score (Fig. 2B).

164 **The extended N-terminus of chlamydial MreB is sufficient to direct an *E. coli* MreB**
165 **lacking its amphipathic helix to the membrane.** Although aa1-23 of CtrMreB were not able
166 to direct GFP to the membrane, we speculated that its membrane-associating properties may

167 be revealed when fused directly to an EcMreB truncation mutant lacking its amphipathic helix
168 (ΔN7aa EcMreB), which fails to localize at the membrane(9). To test this, we fused the N-
169 terminal region of chlamydial MreB to ΔN7aa EcMreB_GFP (illustrated in Fig. 4D) and
170 observed the localization of these constructs in *E. coli* (Fig. 4E). Wild-type EcMreB_GFP is
171 localized to the membrane whereas ΔN7aa EcMreB_GFP appears as aggregates in the
172 cytosol(9). Both chlamydial aa1-23 and aa1-28 clearly redirected ΔN7aa EcMreB_GFP to the
173 membrane, suggesting that these sequence elements possess amphipathic features sufficient to
174 direct the membrane localization of an MreB homolog (Fig. 4E). From these data, we conclude
175 that the amphipathic helix is important for the membrane localization of MreB and aa1-23 may
176 confer additional membrane binding affinities and/or properties to chlamydial MreB.

177 **The extended N-terminal region of chlamydial MreB is sufficient to direct GFP to the**
178 **membrane in *C. trachomatis* L2.** Given the ability of aa1-23 of chlamydial MreB to direct
179 ΔN7aa EcMreB_GFP to the membrane in *E. coli*, we next asked the question whether this
180 region, alone or in combination with the amphipathic helix (aa24-28), could direct GFP to the
181 membrane directly in *Chlamydia*. The $MreB_{1\text{-}23aa}$_GFP or $MreB_{1\text{-}28aa}$_GFP fusions were moved
182 to an inducible chlamydial expression plasmid and transformed into *C. trachomatis* L2. These
183 transformants were then used to infect HeLa cells, and construct expression was induced at
184 either 6 or 16 hpi. Infected cells were fixed and imaged at 10.5 or 20 hpi, respectively (Fig. 5
185 with additional images in Suppl. Fig. 5). GFP alone is a cytosolic protein when expressed in
186 chlamydiae (Fig. 5A). For both fusion proteins, GFP fluorescence was observed at membrane
187 sites (Fig. 5B&C with arrowheads in 5B indicating individual bacteria with membrane
188 localization of GFP) at both time points examined. We conclude from these data that the
189 extended N-terminal region of chlamydial MreB is sufficient to direct GFP to the membrane in
190 *Chlamydia*.

191 **An N-terminal truncation of MreB shows reduced membrane-localization in *Chlamydia*.**
192 To further investigate the role of the N-terminal region of MreB in *Chlamydia*, we constructed
193 three truncations each fused to a C-terminal hexahistidine tag: one lacking the additional N-
194 terminal region (ΔN22), one lacking both the N-terminal region and the amphipathic helix
195 (ΔN28), and one lacking all high A-score residues as described in Figure 2 (illustrated in Suppl.
196 Fig. 6A). Each MreB_6xH was inducibly expressed directly in *C. trachomatis* L2. Only the
197 ΔN32 MreB_6xH truncation showed reduced membrane binding with more accumulation in
198 the cytosol compared to the other constructs (Suppl. Fig. 6B). An important caveat to these
199 studies is that the endogenous chromosomally encoded MreB is still present as it is not
200 currently possible to generate a reliable conditional knockout in *Chlamydia* (see Discussion).

201 **The extended N-terminal region is dispensable for MreB homo-oligomerization but**
202 **essential for interactions with other division proteins.** Given the caveat noted above, we
203 next asked whether the N-terminal region is necessary for MreB homo-oligomerization. In
204 *E.coli*, MreB interacts with itself to form short filaments(10). In addition, since MreB
205 participates in both cell shape determination and cell division, it interacts with diverse proteins
206 related to cell division and peptidoglycan synthesis(14, 19, 20). These features are shared with
207 chlamydial MreB, which interacts with itself and with several proteins such as the cytoskeletal
208 protein RodZ and the cell division components FtsK and FtsQ(6, 8, 21). Based on these
209 previous reports, we hypothesized that the extended N-terminal region is important for these
210 interactions. To test this, we used the bacterial adenylate cyclase-based two hybrid (BACTH)
211 assay, which is based on the reconstitution of enzyme activity by two interacting proteins that
212 bring catalytic adenylate cyclase fragments (T25 and T18) into close proximity. We designed
213 BACTH constructs encoding truncated MreB mutants and then performed BACTH assays (Fig.
214 6). The N-terminal truncations of MreB interacted with full-length MreB (Fig. 6A and
215 summarized in B), providing a potential explanation for the localization data of MreB_6xH

216 truncations in *Chlamydia* (Suppl. Fig. 6). However, these truncated MreBs did not interact with
217 RodZ, full-length FtsK, or the N-terminal region of FtsK lacking its ATPase domain whereas
218 full-length MreB did interact with these constructs (Fig. 6C and summarized in D)(8, 21). From
219 these data, we conclude that the extended N-terminal region is dispensable for MreB homo-
220 oligomerization but is critical for interacting with other proteins related to cell division.

221 **Discussion**

222 MreB is a well characterized rod-shape determining protein, which is conserved in most
223 bacilli(18). For example, when the *mreB* gene is deleted, the cell shape is changed from bacillus
224 to coccoid in *E.coli*(18). MreB participates primarily in organizing PG synthesis by interacting
225 with other proteins, such as MreC and RodZ, to direct Pbp2 and RodA activity at the
226 membrane(19, 22). Recently, MreB has been observed as a dynamic cytoskeletal protein
227 because it forms short filaments and rotates around the membrane perpendicularly to the
228 longitudinal axis of the cell(11). This motion is driven by PG synthesis and is critical for cell
229 elongation and maintenance of rod shape(23). Given these characteristics and properties of
230 MreB, it is surprising that *Chlamydia*, a Gram-negative coccoid bacterium that lacks PG in its
231 cell wall, encodes MreB. This suggests that the maintenance of cell morphology may not be
232 the primary function of chlamydial MreB(5, 24). Rather, given the function of chlamydial PG
233 strictly in cell division, chlamydial MreB may function in this process.

234 Since *Chlamydia* does not have the conserved cell division organizing protein FtsZ, we have
235 hypothesized and presented evidence that MreB is a functional substitute for FtsZ(6-8, 21).
236 However, this raises the intriguing question of how MreB, which is highly conserved between
237 *Chlamydia* and phylogenetically unrelated bacteria, can serve as the divisome organizer.
238 Interestingly, when MreB is reintroduced into MreB-depleted cells in *B. subtilis*, a budding
239 shape is observed that is enriched in MreB(25). This eventually leads to recruitment of cell

240 wall machinery and formation of a rod-shape. However, in *Chlamydia*, which also undergoes
241 a budding-like polarized division, this process is spatially restricted, thus what prevents
242 *Chlamydia* from continuing to synthesize PG to produce a rod shape? One hypothesis is that
243 chlamydial MreB exhibits a restricted distribution that is at least in part dependent upon its
244 unique structural features, and we have shown here that the unique N-terminal region of
245 chlamydial MreB can facilitate the membrane association of this cytoskeletal protein.

246 To initiate this study, we attempted to localize endogenous chlamydial MreB using an antibody
247 previously described(13). Prior reports suggested that MreB is localized as puncta at sites of
248 division(13, 16). Our goal was to capture MreB localization at high resolution and at early
249 stages of division since it becomes more difficult to resolve individual organisms within the
250 inclusion as RBs multiply. However, we were unable to detect endogenous MreB using the
251 previously reported antibody. We, therefore, took advantage of genetic tools that have been
252 recently developed for *Chlamydia* to transform this bacterium with a plasmid construct
253 encoding an inducible MreB_6xH. Using this strategy, we detected MreB_6xH localized at the
254 division septum during the polarized division of the first RB. More interestingly, MreB formed
255 a ring at the septum in the dividing cell that resembled the FtsZ-ring at the septum of *E. coli*
256 (Fig.1). The septal MreB ring is very similar to the PG ring previously observed in
257 *Chlamydia*(5). We speculate that the MreB puncta previously observed may be due to the low
258 affinity of the MreB antibody as we were also unable to detect MreB at later stages during
259 infection using this reagent. Given the effects of inhibiting MreB activity on chlamydial
260 division and PG synthesis(7, 8, 16), these data further suggest that chlamydial MreB likely has
261 a scaffolding function for cell divisome proteins to direct PG synthesis in a manner similar to
262 the function of FtsZ in *E.coli*(26).

263 To further investigate how chlamydial MreB may substitute for FtsZ in *Chlamydia*, we

264 performed a simple alignment of MreB homologs from *Chlamydia* species and other rod-shape
265 bacteria. Many Gram-negative MreB homologs possess an amphipathic helix at their N-
266 terminus that allows MreB to associate with the inner membrane(9). *Chlamydia* species have
267 conserved this feature. The most striking difference between the chlamydial species and other
268 "canonical" MreB homologs is the presence of an extended N-terminus of 23 amino acids (aa1-
269 23). Amphipathic prediction algorithms suggested this region possesses amphipathicity.
270 Interestingly, canonical MreB filaments are excluded from areas of high membrane curvature
271 in bacilli that are typically enriched in anionic phospholipids such as cardiolipin (i.e. the cell
272 poles(27)), but *Chlamydia* are coccoid with its membrane displaying curvature similar to the
273 poles of bacilli. Therefore, we hypothesized that the additional residues at the N-terminus of
274 chlamydial MreB may allow it to associate more efficiently with membranes that exhibit
275 curvature. In addition, these residues may be critical for establishing polarity in this organism
276 as we previously observed that inhibiting MreB activity with A22 or MP265 not only blocks
277 cell division but also depolarizes the RB(7, 8).

278 The amphipathic helix of canonical Gram-negative MreB homologs is critical for the
279 association of MreB with membranes. This was demonstrated by two means: expressing two
280 copies of the helix in tandem fused to the N-terminus of GFP and deleting the helix from MreB
281 and assessing its localization(9). In the former, GFP was directed to the inner membrane(9). In
282 the latter, MreB is no longer localized as membrane patches but rather as cytosolic aggregates
283 in *E. coli*(9). Using the former approach, we observed that two copies, but not one copy, of the
284 chlamydial amphipathic helix were sufficient to direct MreB to the membrane, consistent with
285 what has been observed in *E. coli* (Fig. 4B). However, the additional N-terminal region of
286 chlamydial MreB (aa1-23) together with a single copy of the helix (aa24-28) directed GFP to
287 the membrane. Intriguingly, the membrane localization was restricted to the cell polar region
288 but did not appear as an inclusion body. These data suggest that the additional N-terminal

289 region (aa1-23) can direct membrane localization and may possess affinity for regions of high
290 membrane curvature. Yet, this region alone or in two copies was not sufficient to direct GFP to
291 the membrane. This may indicate that the membrane affinity of this N-terminal region is
292 context specific. Therefore, we tested if it was capable of redirecting an *E. coli* truncation
293 mutant of MreB, lacking its amphipathic helix, to the membrane. This was the case. Therefore,
294 we conclude that the additional N-terminal region of chlamydial MreB encodes a membrane-
295 targeting function. Indeed, this was supported by the ability of this region to direct GFP to the
296 membrane when expressed in *Chlamydia* directly. We propose that chlamydial MreB, with both
297 its extended N-terminus and amphipathic helix, may be more tightly associated with
298 membranes and is critical for it to form ring structures associated with regions of high
299 membrane curvature. We are currently working to prepare recombinant protein of full-length
300 and truncated chlamydial MreB to test this in liposomes.

301 As *Chlamydia* is an obligate intracellular bacterium, it is time-consuming and difficult to
302 genetically modify its genes in a targeted manner, and there is a high failure rate in doing so.
303 Ideally, we would create a conditional knockout such that we could express truncated mutants
304 of chlamydial MreB in the absence of the chromosomal full-length copy. We did attempt to
305 localize truncation mutants of MreB in *Chlamydia*, but only the mutant lacking all predicted
306 amphipathicity showed a different profile. The truncations lacking the extended N-terminus
307 (aa1-23) and both that region and the amphipathic helix (aa1-28) still showed membrane
308 localization (Suppl. Fig. 6). While the mutant lacking all predicted amphipathicity (aa1-32)
309 appeared more cytosolic than the other constructs, some signal was detected at the membrane.
310 Not surprisingly, we detected interactions between the MreB truncations and the full-length
311 MreB, thus one interpretation is that the truncations, when expressed in *Chlamydia*, interacted
312 with full-length MreB (Fig. 6), which is itself at the membrane. In *E.coli*, the residues, V121
313 and S284, participate in forming the protofilament of MreB, and chlamydial MreB possesses

314 similar residues, V139 and A302, respectively(28). Furthermore, the N-terminal region is
315 important for interactions with other proteins related to cell division and PG synthesis. When
316 the region was deleted, chlamydial MreB no longer interacted with RodZ and FtsK by bacterial
317 two-hybrid analysis. One possible explanation of these data is that the truncated MreB isoforms
318 do not associate with the membrane efficiently enough to interact with the membrane proteins
319 RodZ and FtsK. Nevertheless, these data suggest the extended N-terminal region may function
320 as a scaffolding platform for MreB to interact with other proteins related to cell division and
321 may be crucial for the cell divisome formation at the septum, like FtsZ.

322 The sequence similarity between chlamydial MreB and *E.coli* MreB is 71%, and we previously
323 observed that these homologs will interact by two-hybrid analysis(6, 21). Therefore, we tested
324 whether chlamydial MreB could functionally complement an *E. coli mreB* deletion strain.
325 Given the differences at the N-terminus and the role of MreB as part of a multicomponent
326 machinery that directs cell wall synthesis, it is perhaps not surprising that chlamydial MreB
327 failed to complement an *E. coli mreB* mutant strain even when the additional N-terminal region
328 was removed (Fig. 3). To date, we have been unable to complement any structural components
329 of the *E. coli* divisome (e.g. FtsQ(6)) or Mre system (MreB or RodZ(21)), which reinforces the
330 importance of recapitulating all necessary interactions to efficiently complement. In contrast,
331 cytosolic components of the PG synthesis pathway possessing enzymatic activity have been
332 shown to complement *E. coli* conditional mutants(29-31). These data are consistent with the
333 notion that the PG synthesis machinery is conserved in these organisms but the mechanisms by
334 which PG is used and directed are not.

335 Outstanding questions remain: how is polarity established in *Chlamydia*? Is it MreB-dependent
336 or are other factors involved? Is MreB actively excluded from other parts of the membrane by
337 an unknown system similar to the function of the MinCDE system in restricting FtsZ to division

338 septa during binary fission? These are active areas of investigation in our labs and are of great
339 interest to the community. In this study, we performed the first systematic investigation of
340 chlamydial MreB and its function as a cell division coordinator. Our data suggest that
341 chlamydial MreB has multiple membrane-associating domains that may promote its assembly
342 at the septum. This in turn may allow it to functionally substitute for the role of FtsZ in
343 organizing the division septum.

344

345 Materials and Methods

346 Organisms and Cell Culture

347 McCoy (kind gift of Dr. Harlan Caldwell) and HeLa (ATCC, Manassas, VA) cells were cultured
348 at 37°C with 5% CO_2 in Dulbecco's Modified Eagle Medium (DMEM; Invitrogen, Waltham,
349 MA) containing 10% fetal bovine serum (FBS; Hyclone, Logan, UT) and 10 µg/mL gentamicin
350 (Gibco, Waltham, MA). *Chlamydia trachomatis* serovar L2 (strain 434/Bu) lacking the
351 endogenous plasmid (-pL2) was infected and propagated in McCoy cells for use in
352 transformations. HeLa cells were infected with chlamydial transformants in DMEM containing
353 10% FBS, 10 µg/mL gentamicin, 1 U/mL penicillin G, and 1 µg/mL cycloheximide. All cell
354 cultures and chlamydial stocks were routinely tested for *Mycoplasma* contamination using the
355 Mycoplasma PCR detection kit (Sigma, St. Louis, MO). For *E.coli*, wild-type MG1655 and the
356 *mreB*-deficient strain P2733 (kind gift of Dr. Piet de Boer) were cultured at 37°C with 225 rpm
357 shaking in Lysogeny broth (LB) media containing no or several antibiotics as indicated: 50
358 µg/mL spectinomycin, 34 µg/mL chloramphenicol, or 25 µg/mL tetracycline. All chemicals
359 and antibiotics were obtained from Sigma unless otherwise noted.

360 Cloning

361 The plasmids and primers used in this study are described in Supplemental Table 1. The wild-
362 type and truncated *Chlamydia trachomatis mreB* genes were amplified by PCR with Phusion
363 DNA polymerase (NEB, Ipswich, MA) using 100 ng *C. trachomatis* L2 genomic DNA as a
364 template. Some gene segments were directly synthesized as a gBlock fragment (Integrated
365 DNA Technologies, Coralville, IA). The PCR products were purified using a PCR purification
366 kit (Qiagen, Hilden, Germany). The HiFi Assembly reaction master mix (NEB) was used
367 according to the manufacturer's instructions in conjunction with plasmids pASK-GFP-
368 mKate2-L2 (kind gift of Dr. P. Scott Hefty) cut with FastDigest AgeI and EagI (Thermofisher,
369 Waltham, MA), pBOMB4-Tet (kind gift of Dr. Ted Hackstadt) cut with EagI and KpnI, pKT25
370 or pUT18C cut with BamHI and EcoRI, or pBAD33 cut with XbaI and SalI depending on the
371 construct being prepared. All plasmids were also dephosphorylated with FastAP
372 (ThermoFsher). The products of the HiFi reaction were transformed into either NEB-10beta
373 (for chlamydial transformation plasmids) or DH5alpha (I^q) competent cells (NEB), plated on
374 appropriate antibiotics, and plasmids were subsequently isolated from individual colonies
375 grown overnight in LB broth by using a mini-prep kit (Qiagen). For chlamydial transformation,
376 the constructs were transformed into *dam*$^-$ *dcm*$^-$ competent cells (NEB) and purified as de-
377 methylated constructs.

378 **Bioinformatics Analysis**

379 Sequences for *Chlamydia trachomatis* serovar L2/434, *Pseudomonas aeruginosa* (PAO1), and
380 *Vibrio cholerae* (O395) were obtained from the NCBI database (https://www.ncbi.nlm.nih.gov/)
381 and for *E.coli* MG1655 from Ecocyc database (https://ecocyc.org/)(32). Protein sequence
382 alignment was performed using Clustal Omega website
383 (https://www.ebi.ac.uk/Tools/msa/clustalo/)(33) and the ESPript3 program
384 (http://espript.ibcp.fr)(34). Helical wheels were made by using Helixator

385 (http://www.tcdb.org/progs/helical_wheel.php)(35). Amphipathic helixes were predicted by
386 using Amphipaseek program (https://npsa-prabi.ibcp.fr/cgi-
387 bin/npsa_automat.pl?page=/NPSA/npsa_amphipaseek.html)(36).

388 **Transformation of *Chlamydia trachomatis***

389 McCoy cells were plated in a six-well plate the day before beginning the transformation
390 procedure. *Chlamydia trachomatis* serovar L2 without plasmid (-pL2) (kind gift of Dr. Ian
391 Clarke) was incubated with 2 µg demethylated plasmid in Tris-$CaCl_2$ buffer (10 mM Tris-Cl,
392 50 mM $CaCl_2$) for 30 min at room temperature. During this step, the McCoy cells were washed
393 with 2 mL Hank's Balanced Salt Solution (HBSS) media containing Ca^{2+} and Mg^{2+} (Gibco).
394 After that, McCoy cells were infected with the transformants in 2 mL HBSS per well. The plate
395 was centrifuged at 400 *x g* for 15 min at room temperature and incubated at 37°C for 15 min.
396 The inoculum was aspirated, and DMEM containing 10% FBS and 10 µg/mL gentamicin was
397 added per well. At 8 h post infection (hpi), the media was changed to media containing 1 µg/mL
398 cycloheximide and 1 or 2 U/mL penicillin G, and the plate was incubated at 37°C until 48 hpi.
399 At 48 hpi, the transformants were harvested and used to infect a new McCoy cell monolayer.
400 These harvest and infection steps were repeated every 48 hpi until mature inclusions were
401 observed.

402 **Complementation assay**

403 The arabinose-inducible vectors encoding nothing, *E. coli* MreB, chlamydial MreB, or ΔN22
404 chlamydial MreB were transformed in both wild-type (MG1655) and *mreB* mutant strain
405 (P2733; kind gift of Dr. Piet de Boer). Chemically competent cells of each strain were prepared
406 using standard techniques with $CaCl_2$. The strains were cultured overnight, diluted 1/50 in LB
407 media containing chloramphenicol (34 µg/mL), tetracycline (25 µg/mL) or spectinomycin (50

408 μg/mL) and cultured for 2 hours when 0.01% arabinose was added as an inducer or cells were
409 left uninduced as a control. After 2 hours and 6 hours of induction, 4 μL of the cells were
410 mounted on 1% LB agar pad and covered with a cover slip. The morphologies of the strains
411 were observed by a Zeiss Imager.Z2 equipped with an Apotome2 using a 100X objective.

412 **The localization of chlamydial MreB fusion proteins in *E. coli***

413 The *E.coli* MG1655 wild-type and Δ*mreB* mutant (P2733) transformed with the arabinose-
414 inducible vectors encoding GFP with various MreB N-terminal peptides were cultured at 37°C
415 with 255 rpm shaking overnight. Overnight cultures were diluted 1:100 (MG1655) or 1:50
416 (P2733) in LB media containing appropriate antibiotics and cultured at 37°C with 255 rpm
417 shaking. After 2 hours of shaking, the cells were induced, or not, with 0.05% (w/v) arabinose
418 and cultured for more 2 hours. Before mounting the samples, SynaptoRed-C2 (FM4-64;
419 Cayman Chemical, Ann Arbor, MI) was added in the samples to a final concentration 1.5 μM
420 to stain the membrane. After 15 min, 4 μL of each culture were placed on 1% LB agar pad and
421 covered with coverslip. The samples were observed with a Zeiss Imager.Z2 equipped with an
422 Apotome2 using a 100X objective.

423 **Indirect Immunofluorescence (IFA) Microscopy**

424 HeLa cells were seeded in 24-well plates on coverslips at a density of 10^5 cells per well the day
425 before infection. Chlamydial strains expressing wild-type or truncated MreBs with a six-
426 histidine tag at the C-terminus were used to infect HeLa cells in DMEM media containing
427 penicillin G and cycloheximide. At 6 hpi, 10 nM anhydrotetracycline (aTc) was added. At 10.5
428 hpi, the coverslips of infected cells were washed with DPBS and fixed with fixing solution
429 (3.2% formaldehyde and 0.022% glutaraldehyde in DPBS) for 2 min. The samples were then
430 washed three times with DPBS and permeabilized with ice-cold 90% methanol for 1 min.

431 Afterwards, the fixed cells were labeled with primary antibodies including goat anti-major
432 outer-membrane protein (MOMP; Meridian, Memphis, TN), rabbit anti-$MreB_{CT}$ antibody
433 (custom anti-peptide antibody directed against the C-terminus of *C. trachomatis* serovar L2
434 MreB; ThermoFisher), rabbit anti-Hsp60 (kind gift of Dr. Rick Morrison), mouse and rabbit
435 anti-six histidine tag (Genscript, Nanjing, China and Abcam, Cambridge, UK, respectively).
436 Secondary antibodies donkey anti-goat antibody (594), donkey anti-rabbit antibody (647), and
437 donkey anti-mouse (488) were used to visualize the primary antibodies. The secondary
438 antibodies were obtained from Invitrogen. Coverslips were observed by using either a Zeiss
439 LSM 800 confocal microscope or a super-resolution SIM scope (Zeiss ELYRA PS.1).

440 **BACTH Assay**

441 Competent DHT1 *E. coli*, an adenylate cyclase-deficient strain, were co-transformed with
442 pKT25 and pUT18C vectors encoding the genes of interest or empty vectors and spread on
443 M63 minimal media plates containing 50 μg/mL ampicillin, 25 μg/mL kanamycin, 0.5 mM
444 IPTG, 40 μg/mL X-gal, 0.04% casamino acid, and 0.2% maltose. The plates were incubated at
445 30℃ for 5-7 days. Blue colonies indicate positive interactions whereas no growth or small
446 white colonies indicate no interactions.

447 **Acknowledgments**

448 The authors would like to thank Dr. Lisa Rucks for critical review of the manuscript. The
449 authors would like to thank the following individuals for providing reagents used in this study:
450 Dr. Harlan Caldwell (National Institute of Health), Dr. Ian Clarke (University of Southampton),
451 Dr. Piet de Boer (Case Western University), Dr. Ted Hackstadt (Rocky Mountain Labs/NIH),
452 Dr. P. Scott Hefty (University of Kansas), and Dr. Rick Morrison (University of Arkansas for
453 Medical Sciences). This work was supported by a grant from the National Institute for General

454 Medical Science (R35GM124798-01) within the National Institutes of Health to SPO. The
455 University of Nebraska Medical Center Advanced Microscopy Core Facility receives partial
456 support from the National Institute for General Medical Science INBRE - P20 GM103427 and
457 COBRE - P30 GM106397 grants, as well as support from the National Cancer Institute (NCI)
458 for The Fred & Pamela Buffett Cancer Center Support Grant- P30 CA036727 and the Nebraska
459 Research Initiative.

460 **References**

461 1. Abdelrahman YM, Belland RJ. 2005. The chlamydial developmental cycle. FEMS
462 Microbiol Rev 29:949-59.
463 2. Moore ER, Ouellette SP. 2014. Reconceptualizing the chlamydial inclusion as a
464 pathogen-specified parasitic organelle: an expanded role for Inc proteins. Front Cell
465 Infect Microbiol 4:157.
466 3. Stephens RS, Kalman S, Lammel C, Fan J, Marathe R, Aravind L, Mitchell W, Olinger
467 L, Tatusov RL, Zhao Q, Koonin EV, Davis RW. 1998. Genome sequence of an obligate
468 intracellular pathogen of humans: Chlamydia trachomatis. Science 282:754-9.
469 4. Bi EF, Lutkenhaus J. 1991. FtsZ ring structure associated with division in Escherichia
470 coli. Nature 354:161-4.
471 5. Liechti GW, Kuru E, Hall E, Kalinda A, Brun YV, VanNieuwenhze M, Maurelli AT.
472 2014. A new metabolic cell-wall labelling method reveals peptidoglycan in Chlamydia
473 trachomatis. Nature 506:507-10.
474 6. Ouellette SP, Rueden KJ, AbdelRahman YM, Cox JV, Belland RJ. 2015. Identification
475 and Partial Characterization of Potential FtsL and FtsQ Homologs of Chlamydia. Front
476 Microbiol 6:1264.
477 7. Abdelrahman Y, Ouellette SP, Belland RJ, Cox JV. 2016. Polarized Cell Division of
478 Chlamydia trachomatis. PLoS Pathog 12:e1005822.
479 8. Ouellette SP, Karimova G, Subtil A, Ladant D. 2012. Chlamydia co-opts the rod shape-
480 determining proteins MreB and Pbp2 for cell division. Mol Microbiol 85:164-78.
481 9. Salje J, van den Ent F, de Boer P, Lowe J. 2011. Direct membrane binding by bacterial
482 actin MreB. Mol Cell 43:478-87.
483 10. Srinivasan R, Mishra M, Murata-Hori M, Balasubramanian MK. 2007. Filament

484 formation of the Escherichia coli actin-related protein, MreB, in fission yeast. Curr Biol
485 17:266-72.
486 11. van Teeffelen S, Wang S, Furchtgott L, Huang KC, Wingreen NS, Shaevitz JW, Gitai
487 Z. 2011. The bacterial actin MreB rotates, and rotation depends on cell-wall assembly.
488 Proc Natl Acad Sci U S A 108:15822-7.
489 12. Strahl H, Burmann F, Hamoen LW. 2014. The actin homologue MreB organizes the
490 bacterial cell membrane. Nat Commun 5:3442.
491 13. Kemege KE, Hickey JM, Barta ML, Wickstrum J, Balwalli N, Lovell S, Battaile KP,
492 Hefty PS. 2015. Chlamydia trachomatis protein CT009 is a structural and functional
493 homolog to the key morphogenesis component RodZ and interacts with division septal
494 plane localized MreB. Mol Microbiol 95:365-82.
495 14. Bendezu FO, Hale CA, Bernhardt TG, de Boer PA. 2009. RodZ (YfgA) is required for
496 proper assembly of the MreB actin cytoskeleton and cell shape in E. coli. EMBO J
497 28:193-204.
498 15. Swulius MT, Jensen GJ. 2012. The helical MreB cytoskeleton in Escherichia coli
499 MC1000/pLE7 is an artifact of the N-Terminal yellow fluorescent protein tag. J
500 Bacteriol 194:6382-6.
501 16. Liechti G, Kuru E, Packiam M, Hsu YP, Tekkam S, Hall E, Rittichier JT,
502 VanNieuwenhze M, Brun YV, Maurelli AT. 2016. Pathogenic Chlamydia Lack a
503 Classical Sacculus but Synthesize a Narrow, Mid-cell Peptidoglycan Ring, Regulated
504 by MreB, for Cell Division. PLoS Pathog 12:e1005590.
505 17. Wang S, Arellano-Santoyo H, Combs PA, Shaevitz JW. 2010. Actin-like cytoskeleton
506 filaments contribute to cell mechanics in bacteria. Proc Natl Acad Sci U S A 107:9182-
507 5.
508 18. Bendezu FO, de Boer PA. 2008. Conditional lethality, division defects, membrane
509 involution, and endocytosis in mre and mrd shape mutants of Escherichia coli. J
510 Bacteriol 190:1792-811.
511 19. Fenton AK, Gerdes K. 2013. Direct interaction of FtsZ and MreB is required for septum
512 synthesis and cell division in Escherichia coli. EMBO J 32:1953-65.
513 20. Kruse T, Bork-Jensen J, Gerdes K. 2005. The morphogenetic MreBCD proteins of
514 Escherichia coli form an essential membrane-bound complex. Mol Microbiol 55:78-89.
515 21. Ouellette SP, Rueden KJ, Gauliard E, Persons L, de Boer PA, Ladant D. 2014. Analysis
516 of MreB interactors in Chlamydia reveals a RodZ homolog but fails to detect an

517 interaction with MraY. Front Microbiol 5:279.
518 22. van den Ent F, Johnson CM, Persons L, de Boer P, Lowe J. 2010. Bacterial actin MreB
519 assembles in complex with cell shape protein RodZ. EMBO J 29:1081-90.
520 23. Morgenstein RM, Bratton BP, Nguyen JP, Ouzounov N, Shaevitz JW, Gitai Z. 2015.
521 RodZ links MreB to cell wall synthesis to mediate MreB rotation and robust
522 morphogenesis. Proc Natl Acad Sci U S A 112:12510-5.
523 24. Fox A, Rogers JC, Gilbart J, Morgan S, Davis CH, Knight S, Wyrick PB. 1990.
524 Muramic acid is not detectable in Chlamydia psittaci or Chlamydia trachomatis by gas
525 chromatography-mass spectrometry. Infect Immun 58:835-7.
526 25. Hussain S, Wivagg CN, Szwedziak P, Wong F, Schaefer K, Izore T, Renner LD, Holmes
527 MJ, Sun Y, Bisson-Filho AW, Walker S, Amir A, Lowe J, Garner EC. 2018. MreB
528 filaments align along greatest principal membrane curvature to orient cell wall synthesis.
529 Elife 7.
530 26. Hale CA, de Boer PA. 1997. Direct binding of FtsZ to ZipA, an essential component of
531 the septal ring structure that mediates cell division in E. coli. Cell 88:175-85.
532 27. Kawazura T, Matsumoto K, Kojima K, Kato F, Kanai T, Niki H, Shiomi D. 2017.
533 Exclusion of assembled MreB by anionic phospholipids at cell poles confers cell
534 polarity for bidirectional growth. Mol Microbiol 104:472-486.
535 28. van den Ent F, Izore T, Bharat TA, Johnson CM, Lowe J. 2014. Bacterial actin MreB
536 forms antiparallel double filaments. Elife 3:e02634.
537 29. Hesse L, Bostock J, Dementin S, Blanot D, Mengin-Lecreulx D, Chopra I. 2003.
538 Functional and Biochemical Analysis of Chlamydia trachomatis MurC, an Enzyme
539 Displaying UDP-N-Acetylmuramate:Amino Acid Ligase Activity. Journal of
540 Bacteriology 185:6507-6512.
541 30. McCoy AJ, Maurelli AT. 2005. Characterization of Chlamydia MurC-Ddl, a fusion
542 protein exhibiting D-alanyl-D-alanine ligase activity involved in peptidoglycan
543 synthesis and D-cycloserine sensitivity. Mol Microbiol 57:41-52.
544 31. Patin D, Bostock J, Blanot D, Mengin-Lecreulx D, Chopra I. 2009. Functional and
545 biochemical analysis of the Chlamydia trachomatis ligase MurE. J Bacteriol 191:7430-
546 5.
547 32. Keseler IM, Mackie A, Santos-Zavaleta A, Billington R, Bonavides-Martinez C, Caspi
548 R, Fulcher C, Gama-Castro S, Kothari A, Krummenacker M, Latendresse M, Muniz-
549 Rascado L, Ong Q, Paley S, Peralta-Gil M, Subhraveti P, Velazquez-Ramirez DA,

Weaver D, Collado-Vides J, Paulsen I, Karp PD. 2017. The EcoCyc database: reflecting new knowledge about Escherichia coli K-12. Nucleic Acids Res 45:D543-D550.

33. Madeira F, Park YM, Lee J, Buso N, Gur T, Madhusoodanan N, Basutkar P, Tivey ARN, Potter SC, Finn RD, Lopez R. 2019. The EMBL-EBI search and sequence analysis tools APIs in 2019. Nucleic Acids Res doi:10.1093/nar/gkz268.

34. Robert X, Gouet P. 2014. Deciphering key features in protein structures with the new ENDscript server. Nucleic Acids Res 42:W320-4.

35. Saier MH, Jr., Reddy VS, Tsu BV, Ahmed MS, Li C, Moreno-Hagelsieb G. 2016. The Transporter Classification Database (TCDB): recent advances. Nucleic Acids Res 44:D372-9.

36. Sapay N, Guermeur Y, Deleage G. 2006. Prediction of amphipathic in-plane membrane anchors in monotopic proteins using a SVM classifier. BMC Bioinformatics 7:255.

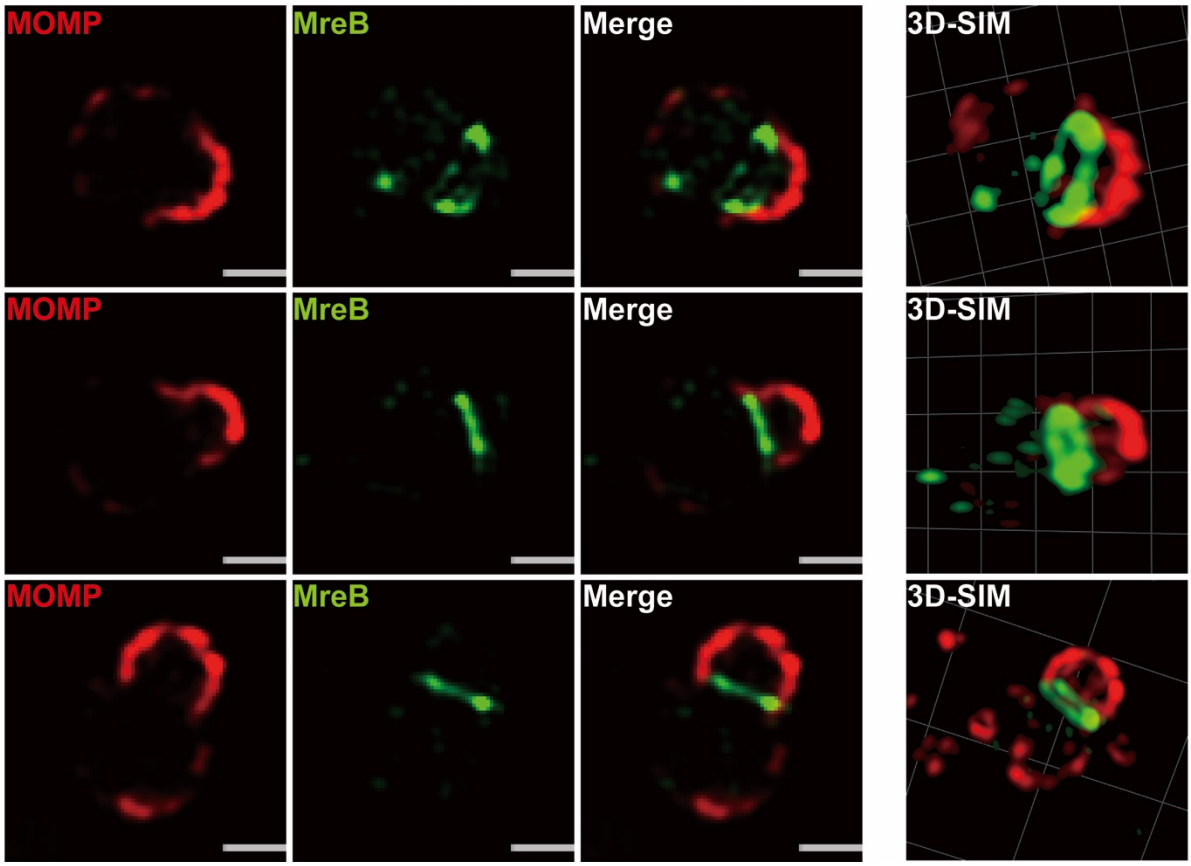

Figure 1. Localization of chlamydial MreB_6xH in *C. trachomatis* using structured illumination microscope (SIM). *C. trachomatis* without plasmid (-pL2) was transformed with anhydrotetracycline (aTc)-inducible vector encoding chlamydial MreB with six histidine tag at the C-terminus. HeLa cells were infected with this strain and chlamydial MreB_6xH expression was induced with 10 nM aTc at 6 hpi. At 10.5 hpi, the infected cells were fixed (3.2% Formaldehyde, 0.022% Glutaraldehyde in PBS) for 2 min and permeabilized with 90% methanol (MeOH) for 1 min. This sample was stained for major outer membrane protein (MOMP; red) and chlamydial MreB (green). Structured illumination microscope (SIM) images were acquired on a Zeiss ELYRA PS.1 super-resolution microscope. The scale bar = 0.5 μm.

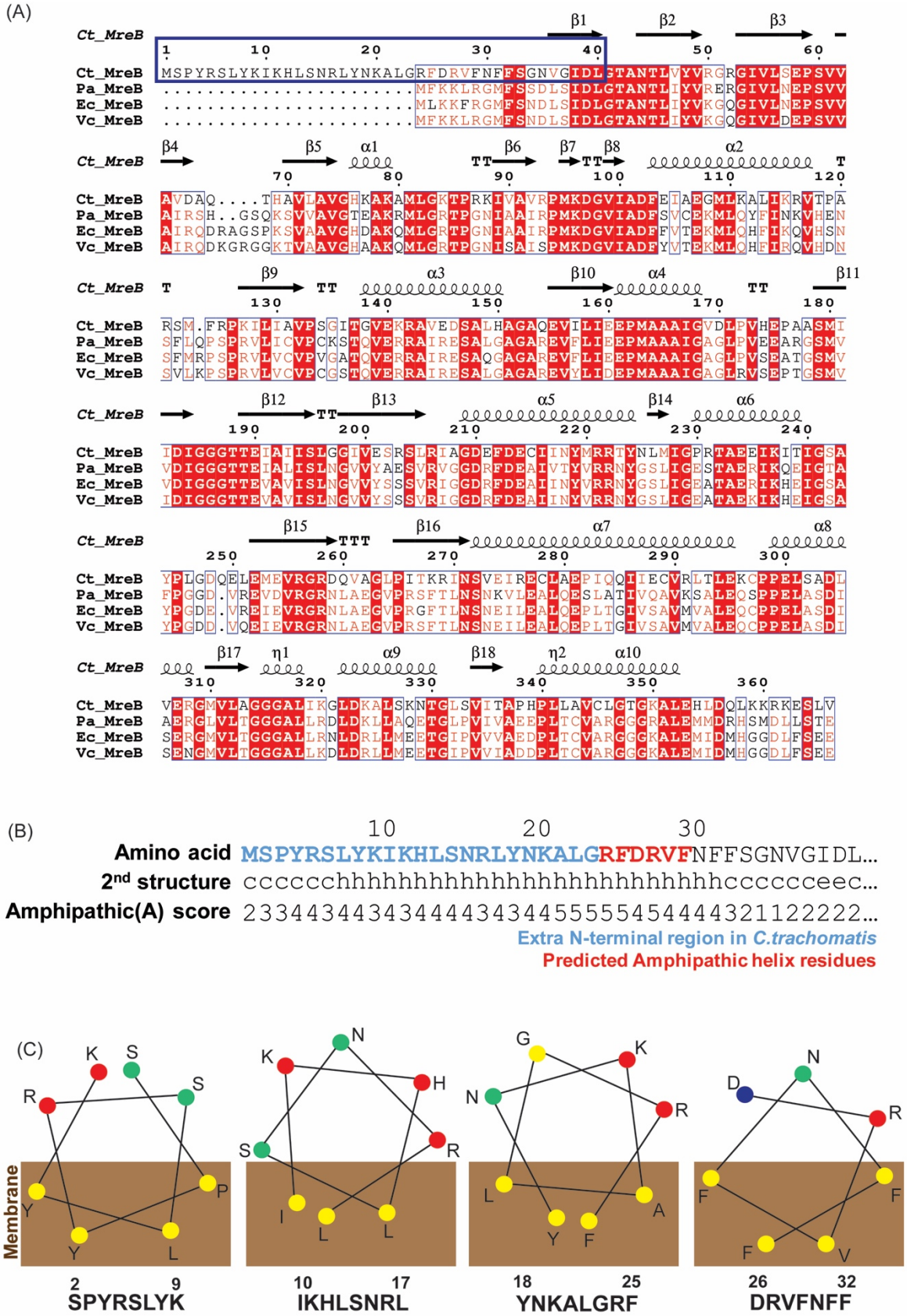

575

576 **Figure 2. Bioinformatics analysis of chlamydial MreB.** Chlamydial MreB has unique

structural features based on the bioinformatics analysis. (A) Protein sequence alignment of chlamydial and other bacterial MreBs. The blue box represents the extended N-terminus and predicted amphipathic helix of chlamydial MreB. The alignment was performed with Clustal Omega (https://www.ebi.ac.uk/Tools/msa/clustalo/) and represented with ESPript 3.0 (http://espript.ibcp.fr). (B) The amphipathic score and the predicted secondary structure of the N-terminus of chlamydial MreB. The prediction of amphipathicity is performed by using AMPHIPASEEK. The blue and red residues represent the extended N-terminus and predicted amphipathic helix, respectively. (C) The amphipathicity of the fragments of the N-terminal region of chlamydial MreB. These amphipathic structures were predicted by online helical wheel program, named Helixator (http://www.tcdb.org/progs/helical_wheel.php). The circles represent residues. (yellow circle: non-polar residue; green circle: uncharged polar residue; red circle: basic polar residue; blue circle: acid polar residue).

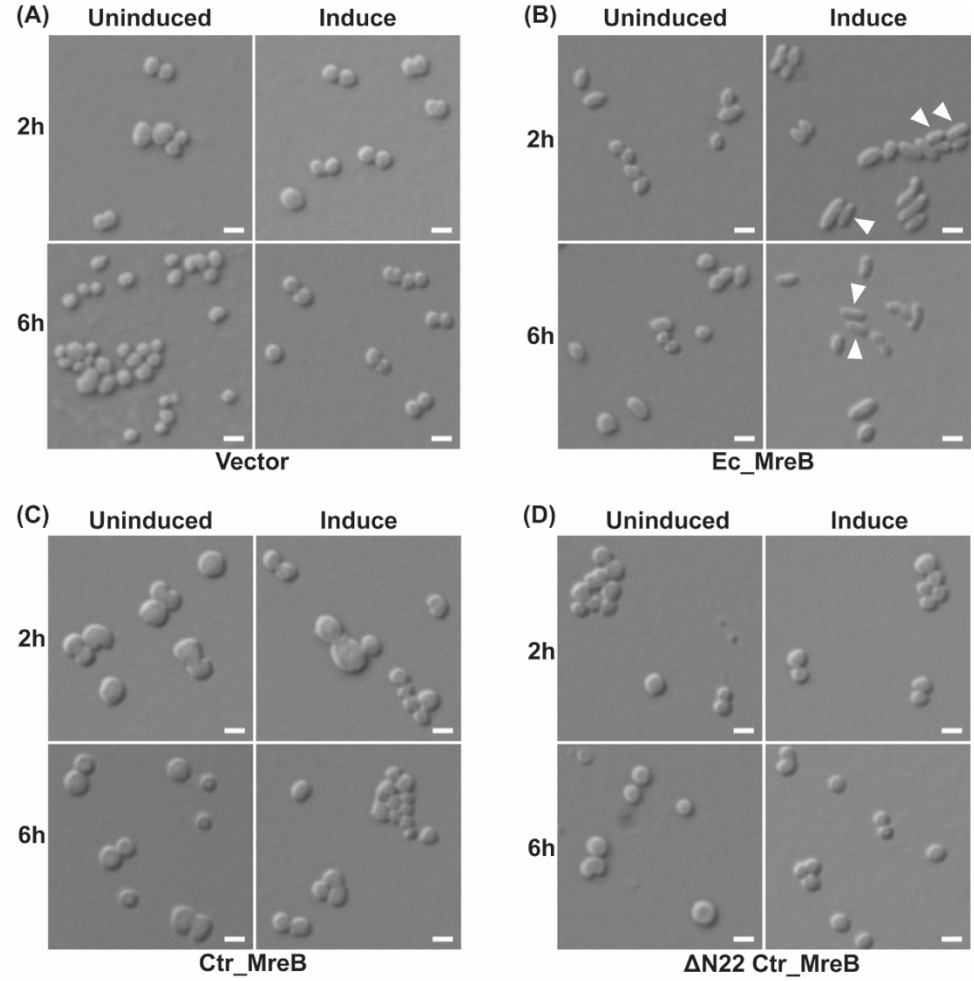

Figure 3. Test of complementation of chlamydial MreB in *E.coli*. An *E.coli* the *mreB*-deficient mutant (P2733) strain was transformed with an empty arabinose-inducible vector (A) and the vectors encoding *E.coli* MreB (B), chlamydial MreB (C) and truncated chlamydial MreB lacking the extended N-terminal region (D). Stationary phase cultures were diluted to 1:50 in LB media containing 50 μg/mL spectinomycin, 25 μg/mL tetracycline, and 34 μg/mL chloramphenicol and cultured at 37℃ with 225 rpm shaking for 2 h. The cells were then induced or not with 0.01% (w/v) arabinose. After induction, 4 μL of each culture at 2 h and 6 h were spotted under a 1% LB agar pad and covered with a coverslip. Images were acquired on a Zeiss Imager.Z2 equipped with an Apotome2 using a 100X objective. The arrows indicate the cells complemented by the induction of *E.coli* MreB. Scale bar = 2 μm.

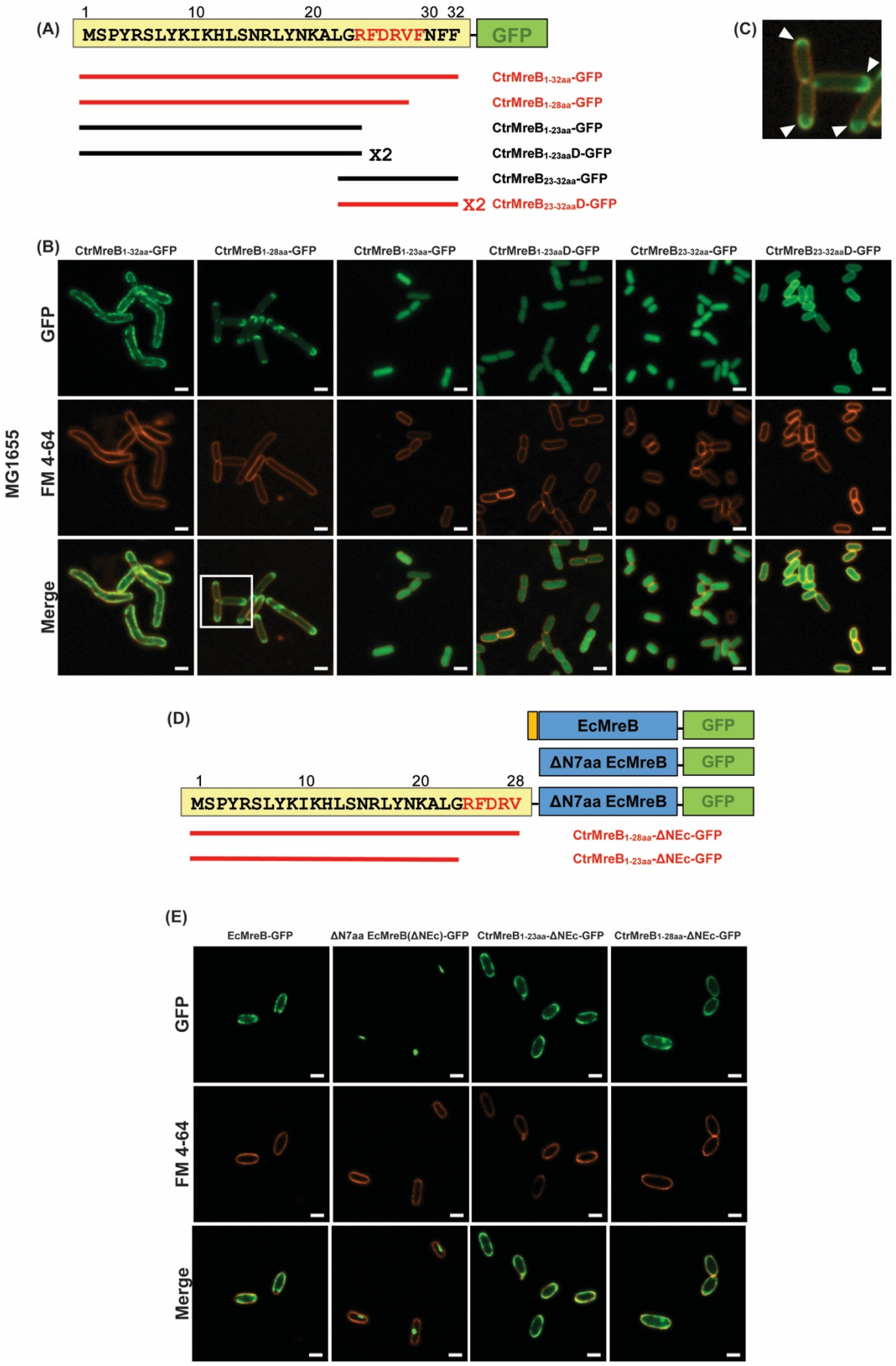
(A)
1
10
20
30 32
MSPYRSLYKIKHLSNRLYNKALGRFDRVFNFF
GFP
CtrMreB1-32aa-GFP
CtrMreB1-28aa-GFP
CtrMreB1-23aa-GFP
X2
CtrMreB1-23aaD-GFP
CtrMreB23-32aa-GFP
X2
CtrMreB23-32aaD-GFP
(C)
(B)
CtrMreB1-32aa-GFP
CtrMreB1-28aa-GFP
CtrMreB1-23aa-GFP
CtrMreB1-23aaD-GFP
CtrMreB23-32aa-GFP
CtrMreB23-32aaD-GFP
GFP
FM 4-64
Merge
MG1655
(D)
EcMreB
GFP
ΔN7aa EcMreB
GFP
1
10
20
28
MSPYRSLYKIKHLSNRLYNKALGRFDRV
ΔN7aa EcMreB
GFP
CtrMreB1-28aa-ΔNEc-GFP
CtrMreB1-23aa-ΔNEc-GFP
(E)
EcMreB-GFP
ΔN7aa EcMreB(ΔNEc)-GFP
CtrMreB1-23aa-ΔNEc-GFP
CtrMreB1-28aa-ΔNEc-GFP
GFP
FM 4-64
Merge

601

602 **Figure 4. Localization in *E.coli* of various N-terminal regions of chlamydial MreB fused**
603 **to GFP.** Wild-type MG1655 *E. coli* were transformed with the arabinose-inducible vectors
604 encoding GFP fusions with various N-terminal regions of chlamydial MreB (A,B) or truncated
605 *E.coli* MreB lacking the amphipathic helix (D,E). Stationary phase cultures strains were diluted
606 1:100 in LB media containing 34 μg/ml chloramphenicol and cultured for 2 h. The cells were
607 then induced or not with 0.05% (w/v) arabinose and cultured for 2 h more. To stain the
608 membrane, SynaptoRed-C2 (FM4-64) was added to the samples at a final concentration of 1.5
609 μM. After 15 min, 4 μL of each culture was spotted under a 1% LB agar pad and covered with
610 a coverslip. The images were acquired on a Zeiss Imager.Z2 equipped with an Apotome2 using
611 a 100X objective. (A) The structure of the various N-terminal MreB-GFP fusion peptides. In
612 the boxed region containing the N-terminus of chlamydial MreB; red residues represent the
613 predicted amphipathic helix residues. Red constructs show the membrane localization and
614 black constructs show cytosolic localization. (B) The localization of various N-terminal regions
615 of chlamydial MreB fused to GFP in MG1655. Note the polar membrane localization of the
616 $MreB_{1\text{-}28aa}$-GFP. Scale bar = 2 μm. (C) A zoomed image of $MreB_{1\text{-}28aa}$-GFP localization
617 represented by the box in (B). The arrowheads represent the polar membrane localization of
618 the $MreB_{1\text{-}28aa}$-GFP. Scale bar = 0.5 μm. (D) The structure of the various N-terminal chlamydial
619 MreB regions fused with truncated *E.coli* MreB lacking the amphipathic helix. The orange
620 region represents the amphipathic helix of *E. coli* MreB, and the red residues are predicted
621 amphipathic helix. (E) The localization of the various N-terminal regions of chlamydial MreB
622 fused to the truncated *E.coli* MreB in MG1655. Scale bar = 2 μm.

623

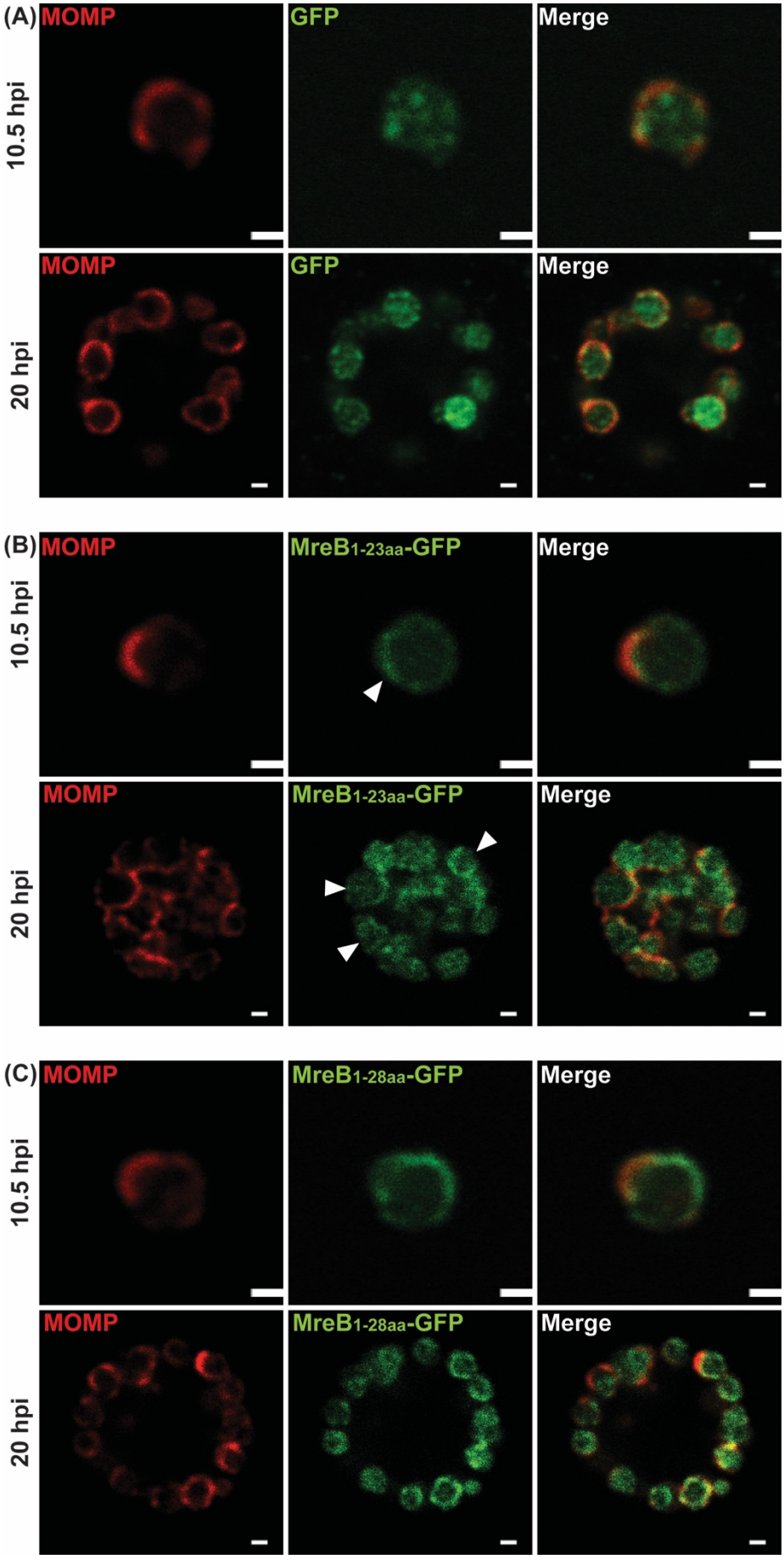
(A)
MOMP
GFP
Merge
10.5 hpi
MOMP
GFP
Merge
20 hpi
(B)
MOMP
MreB1-23aa-GFP
Merge
10.5 hpi
MOMP
MreB1-23aa-GFP
Merge
20 hpi
(C)
MOMP
MreB1-28aa-GFP
Merge
10.5 hpi
MOMP
MreB1-28aa-GFP
Merge
20 hpi

624

625 **Figure 5. Localization in *C. trachomatis* of various N-terminal regions of chlamydial MreB**
626 **fused to GFP.** *C. trachomatis* serovar L2 without plasmid (-pL2) was transformed with
627 anhydrotetracycline (aTc)-inducible vectors encoding GFP (A), chlamydial $MreB_{1\text{-}23aa}$-GFP
628 fusion peptide (B), or chlamydial $MreB_{1\text{-}28aa}$-GFP fusion peptide (C). HeLa cells were infected
629 with the indicated strains, and expression of the GFP fusions was induced at 6 hpi or 16 hpi
630 with 10 nM aTc. At 10.5 hpi or 20 hpi, the samples were fixed (3.2% Formaldehyde, 0.022%
631 Glutaraldehyde in 1X PBS) for 2 min and permeabilized with 90% methanol (MeOH) for 1
632 min. These samples were stained for major outer membrane protein (MOMP; red) with GFP
633 imaged in green. The arrowheads represent the $MreB_{1\text{-}23aa}$-GFP localized at the membrane.
634 Images were acquired on a Zeiss LSM 800 confocal microscope with 63X objective. Scale bar
635 = 0.5 µm (10.5 hpi) or 1 µm (20 hpi).

636

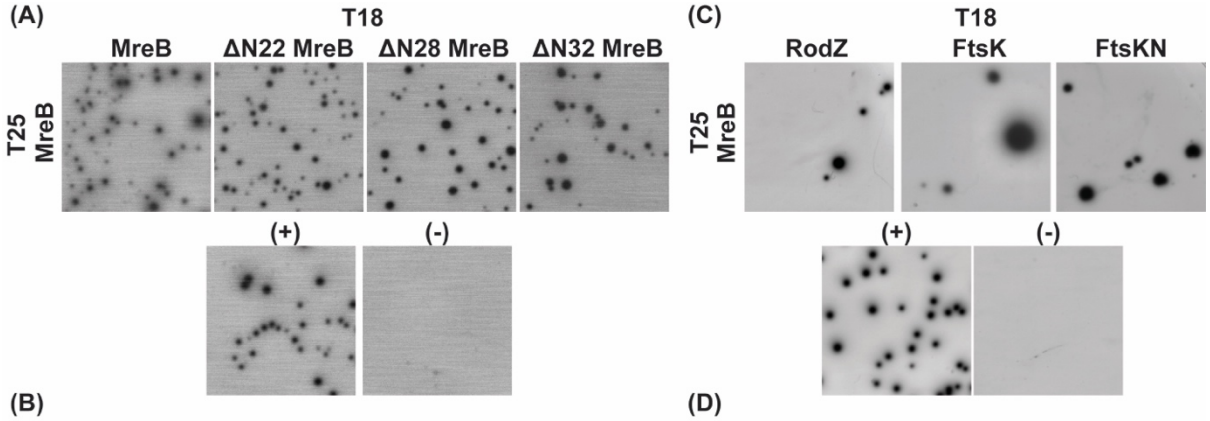

(B)

T25 / T18	MreB	ΔN22 MreB	ΔN28 MreB	ΔN32 MreB
MreB	++++	+++	+	+
ΔN22 MreB	+++	+		
ΔN28 MreB	+++		+	
ΔN32 MreB	+++			+

(D)

T18 / T25	RodZ	FtsK	FtsKN
MreB	++	+	+++
ΔN22 MreB	N/D	N/D	N/D
ΔN28 MreB	N/D	N/D	N/D
ΔN32 MreB	N/D	N/D	N/D

Figure 6. BACTH assay to test protein-protein interactions of full-length and truncated chlamydial MreB. *E.coli* DHT1 (Δ*cya*) was co-transformed with vectors encoding the indicated genes fused to the T25 and T18 catalytic domains of the *B. pertussis* adenylate cyclase. Transformants were plated on M63 minimal medium plates containing 50 µg/mL ampicillin, 25 µg/mL kanamycin, 0.5 mM IPTG, 40 µg/mL X-gal, 0.04% casamino acid, and 0.2% maltose. The plates were incubated at 30℃ for 5-7 days. (A) BACTH assay of the interaction between wild-type and truncated chlamydial MreBs. (B) BACTH assay of the interaction between wild-type or truncated chlamydial MreBs and previously described chlamydial cell division components FtsK, the N-terminal domain of FtsK (FtsKN), and RodZ. A positive (+) control is the interaction between T25-Zip and T18-Zip, the GCN4 leucine zipper motif, and a negative (-) control is the lack of interaction between T25 and the mixture of T18-MreB and T18-ΔN22 MreB. These tests were performed a minimum of two times. Slash box: Not tested; N/D: Non detected.

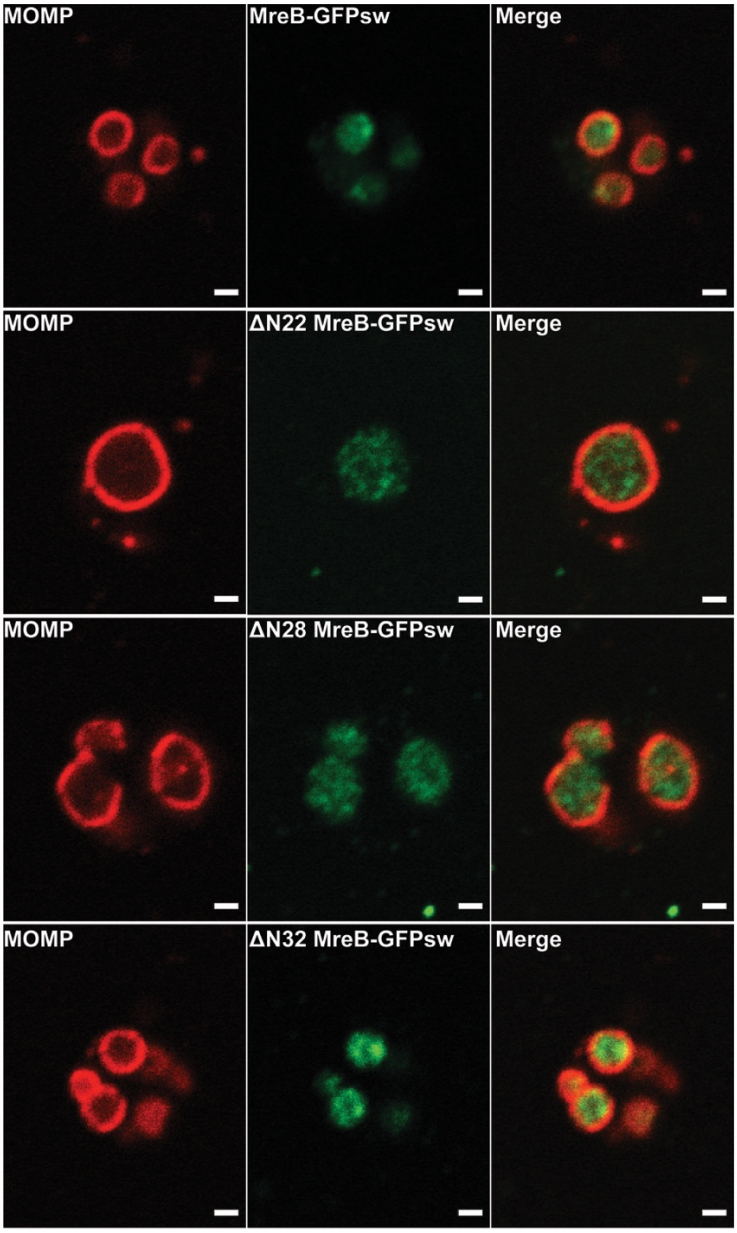

Supplementary figure 1. Localization of chlamydial MreB_GFPsw proteins in *C. trachomatis*. HeLa cells were infected with *C. trachomatis* transformants containing aTc-inducible vectors encoding MreB_GFPsw proteins. At 12 hpi, expression of the GFP sandwich fusions was induced with 10 nM aTc, and the samples were fixed (3.2% Formaldehyde, 0.022% Glutaraldehyde in 1X PBS) at 16 hpi for 2 min and permeabilized with 90% methanol. The samples were stained for major outer membrane protein (MOMP; red) and GFP (green). Images were acquired on a Zeiss LSM 800 confocal microscope. Scale bar = 1 μm

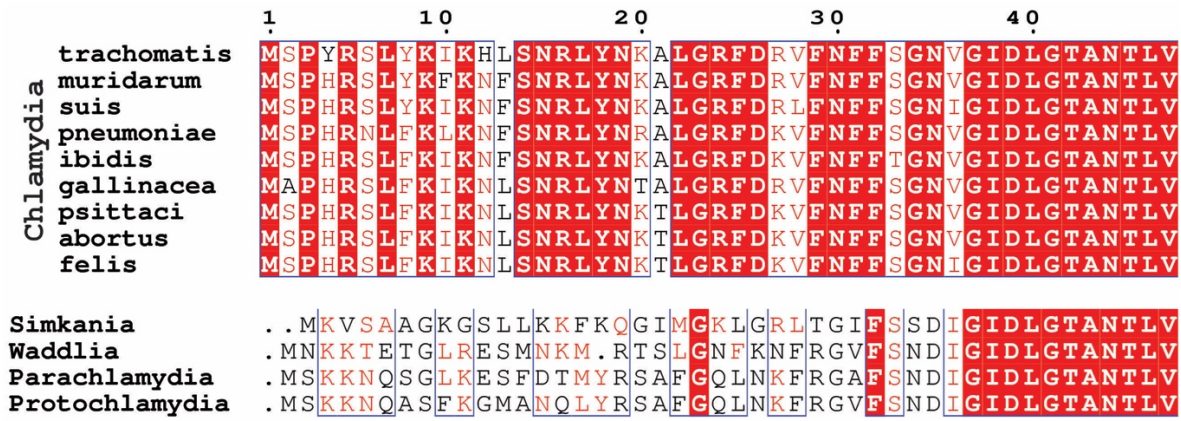

Supplementary figure 2. Protein sequence alignment of the N-terminus of MreB from diverse *Chlamydia* genera. The extended N-terminus of chlamydial MreB is conserved across *Chlamydia*. The alignment was performed with Clustal Omega (https://www.ebi.ac.uk/Tools/msa/clustalo/) and represented with ESPript 3.0 (http://espript.ibcp.fr).

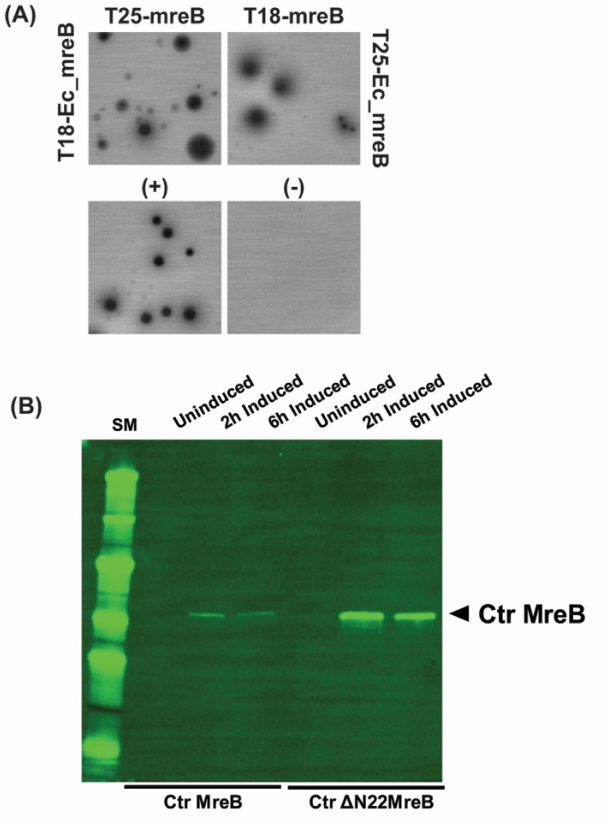

Supplementary figure 3. Interaction between chlamydial and *E. coli* MreBs and the expression of chlamydial MreB in *E. coli.* (A) BACTH assays were carried out to test interactions between chlamydial MreB and *E. coli* MreB. DHT1 *E. coli* were co-transformed with plasmids encoding the indicated fusion proteins and plated on M63 minimal medium containing 50 µg/mL ampicillin, 25 µg/mL kanamycin, 0.5 mM IPTG, 40 µg/mL X-gal, 0.04% casamino acid, and 0.2% maltose. The plates were incubated at 30℃ for 5-7 days. A positive control is the interaction between T25-zip and T18-zip. A negative control is the lack of interaction between T25 and T18-chlamydial MreB and T18-*E. coli* MreB. These tests were performed a minimum of two times. (B) Western blotting was performed to test the expression of chlamydial MreB in strains used in the complementation assay depicted in Figure 3. Whole cell lysates from cultures tested in the complementation assay were separated by SDS-PAGE and transferred to a PVDF membrane. The chlamydial MreB was detected with rabbit anti-MreB primary antibody and IRDye goat anti-rabbit 800CW (LI-COR, Lincoln, NE).

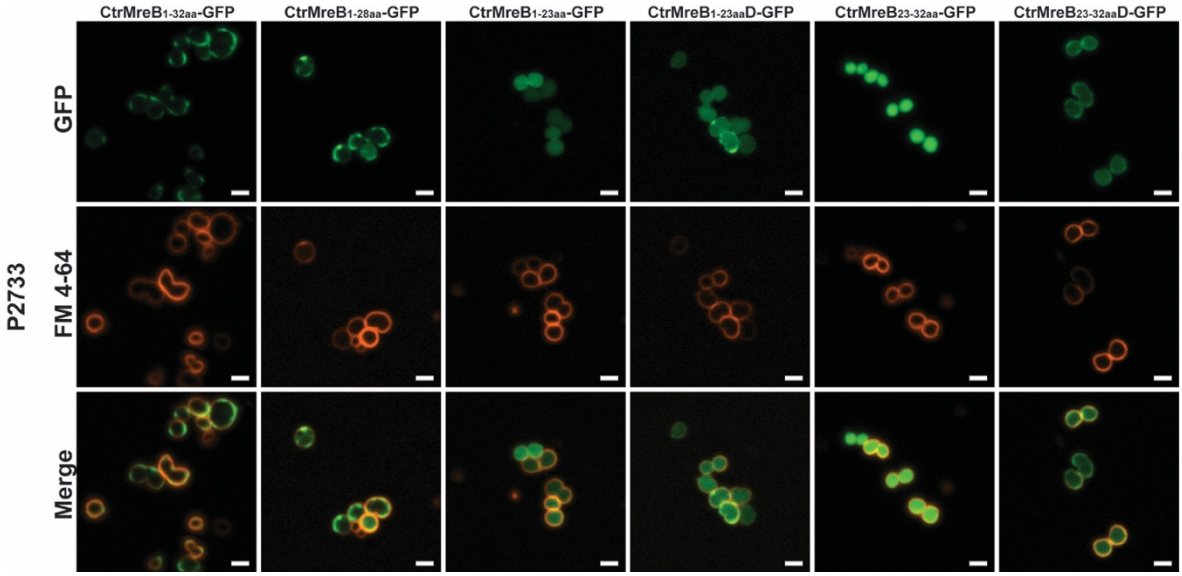

Supplementary figure 4. Localization of N-terminus of chlamydial MreB-GFP fusion proteins in Δ*mreB* mutant (P2733). The Δ*mreB* mutant (P2733) was transformed with the arabinose-inducible vectors encoding GFP fused with diverse N-terminal regions of chlamydial MreB. Samples were prepared as described in the legend to Figure 4 with the membrane labeled with FM4-64. Images were acquired on a Zeiss Imager.Z2 equipped with an Apotome2 using a 100X objective. Scale bar = 2 μm.

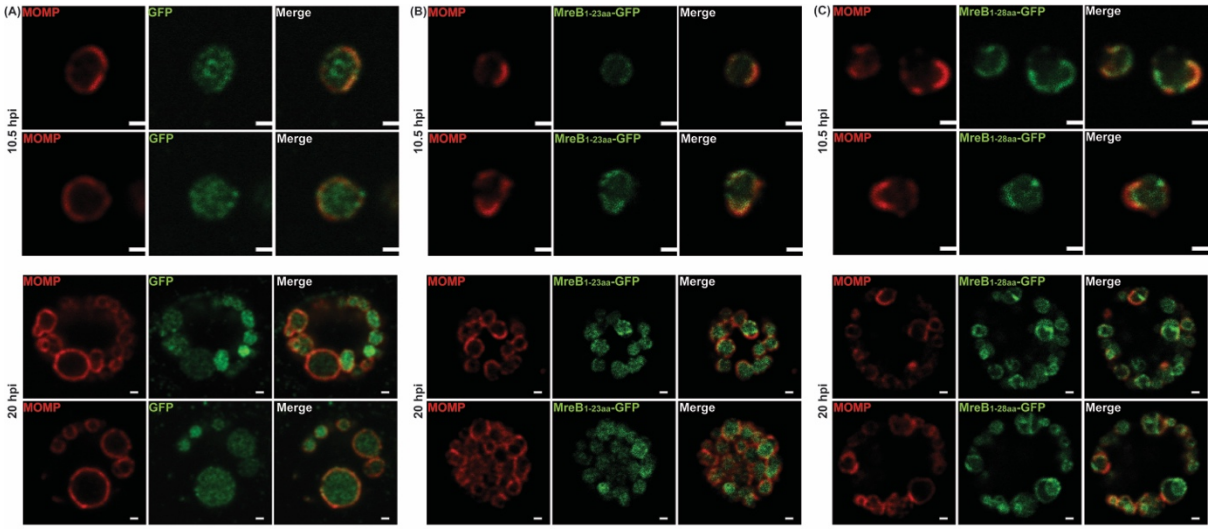

688

689 **Supplementary figure 5. Localization in *C. trachomatis* of various N-terminal regions of**
690 **chlamydial MreB fused to GFP.** *C. trachomatis* without plasmid (-pL2) was transformed with
691 anhydrotetracycline (aTc)-inducible vector encoding GFP (A), chlamydial $MreB_{1\text{-}23aa}$-GFP
692 fusion peptide (B) or chlamydial $MreB_{1\text{-}28aa}$-GFP fusion peptide (C) as described in the legend
693 to Figure 5. These samples were stained for major outer membrane protein (MOMP; red).
694 Images were acquired on a Zeiss LSM 800 confocal microscope with 63X objective. Scale bar
695 = 0.5 µm (10.5 hpi) or 1 µm (20 hpi).

696

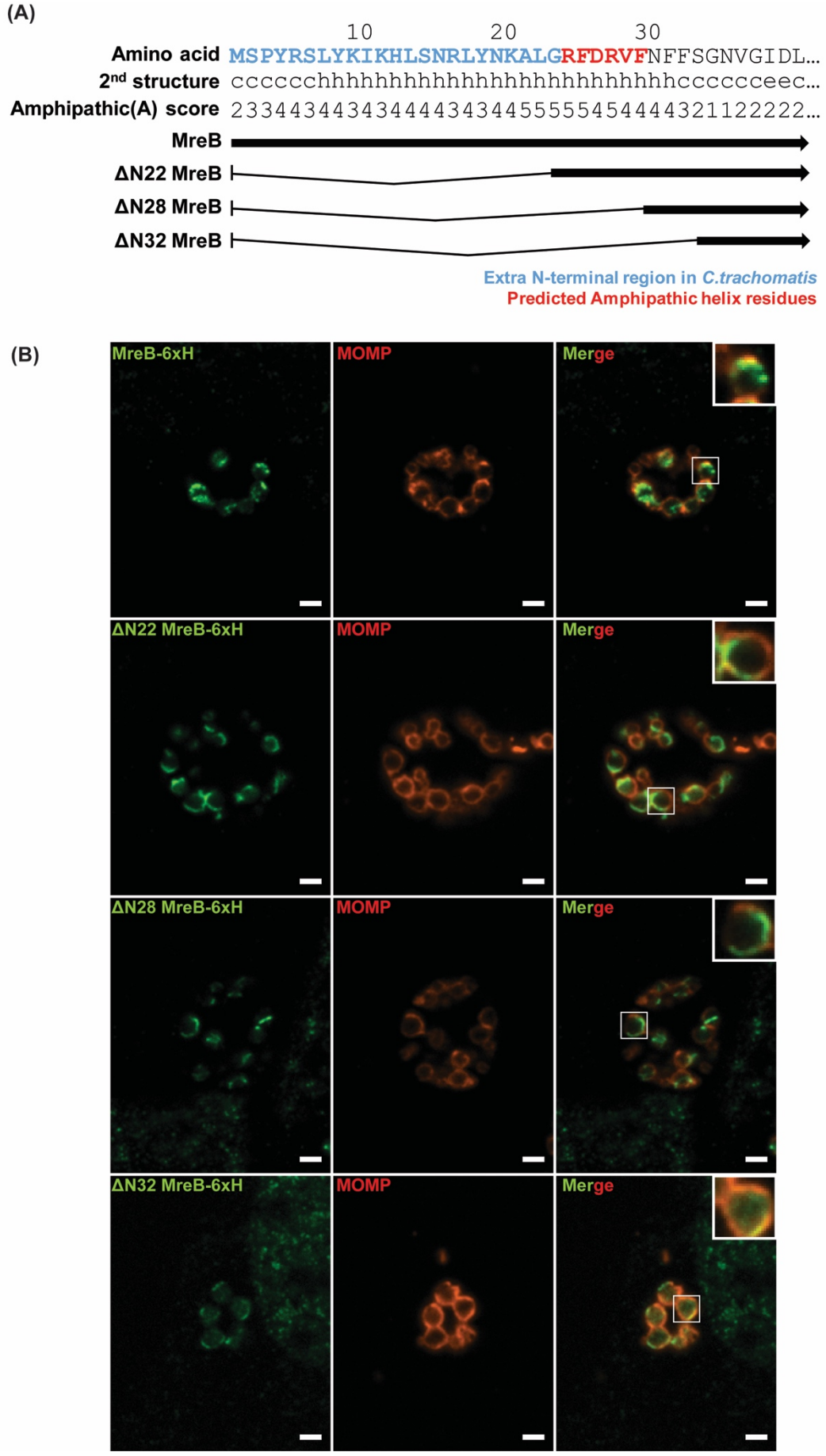
(A)
10 20 30
Amino acid MSPYRSLYKIKHLSNRLYNKALGRFDRVFNFFSGNVGIDL...
2nd structure cccccchhhhhhhhhhhhhhhhhhhhhhhhcccccceec...
Amphipathic(A) score 2334434434344443434455555454444321122222...
MreB
ΔN22 MreB
ΔN28 MreB
ΔN32 MreB
Extra N-terminal region in C.trachomatis
Predicted Amphipathic helix residues
(B)
MreB-6xH
MOMP
Merge
ΔN22 MreB-6xH
MOMP
Merge
ΔN28 MreB-6xH
MOMP
Merge
ΔN32 MreB-6xH
MOMP
Merge

697

698 **Supplementary figure 6. The localization of various truncated chlamydial MreBs in *C.***
699 ***trachomatis* L2.** (A) Representation of the various truncated chlamydial MreBs tested. The
700 blue and red residues represent the extended N-terminus and predicted amphipathic helix,
701 respectively. (B) *C. trachomatis* serovar L2 transformants containing aTc-inducible vectors
702 encoding the truncated MreBs were used to infect HeLa cells. At 16 hpi, expression of the
703 MreB constructs was induced with 10 nM aTc, and these samples were fixed (3.2%
704 Formaldehyde, 0.022% Glutaraldehyde in 1X DPBS) at 20 hpi for 2 min and permeabilized
705 with 90% methanol. The samples were stained for major outer membrane protein (MOMP; red)
706 and six histidine tag (green). Images were acquired on a Zeiss Imager.Z2 equipped with an
707 Apotome2 using a 100X objective. The white box represents the cells which are zoomed in at
708 the upper right. Scale bar = 2 μm

709

710 **Supplementary table 1. The list of Strains, Plasmids and Primers**

Construct Plasmid	Relevant genotype	Ori	Source of Reference
pASK-GFP-mKate-L2 (pTLR2)	*bla* P_{tet}	ColE1	(1)
pTLR2-*mreB*_6xH	*bla* P_{tet}::*Ctr_mreB*_6xH	ColE1	This study
pBAD33	*cat* P_{ara}	p15A	(2)
pBAD33-*Ec_mreB*	*cat* P_{ara}::*Ec_mreB*	p15A	This study
pBAD33-*mreB*	*cat* P_{ara}::*Ctr_mreB*	p15A	This study
pBAD33-*mreB*_67	*cat* P_{ara}::ΔN66nt *Ctr_mreB*	p15A	This study
pBAD33G-*mreB*1-96nt	*cat* P_{ara}::*Ctr_mreB*1-96nt-*gfp*	p15A	This study
pBAD33G-*mreB*1-84nt	*cat* P_{ara}::*Ctr_mreB*1-84nt-*gfp*	p15A	This study
pBAD33G-*mreB*1-69nt	*cat* P_{ara}::*Ctr_mreB*1-69nt-*gfp*	p15A	This study
pBAD33G-*mreB*1-69nt duplicate	*cat* P_{ara}::*Ctr_mreB*1-69nt *Ctr_mreB*1-69nt -*gfp*	p15A	This study
pBAD33G-*mreB*67-96nt	*cat* P_{ara}::*Ctr_mreB*67-96nt-*gfp*	p15A	This study
pBAD33G-*mreB*67-96nt duplicate	*cat* P_{ara}::*Ctr_mreB*67-96nt *Ctr_mreB*67-96nt-*gfp*	p15A	This study
pBAD33G-*Ec_mreB*	*cat* P_{ara}::*Ec_mreB-gfp*	p15A	This study
pBAD33G-*Ec_mreB*_22	*cat* P_{ara}::ΔN21nt *Ec_mreB-gfp*	p15A	This study
pBAD33G-*mreB*1-84nt-*Ec_mreB*_22	*cat* P_{ara}::*Ctr_mreB*1-84nt-ΔN21nt *Ec_mreB-gfp*	p15A	This study
pBAD33G-*mreB*1-69nt-*Ec_mreB*_22	*cat* P_{ara}::*Ctr_mreB*1-69nt-ΔN21nt *Ec_mreB-gfp*	p15A	This study
pBOMB4-Tet	*bla* P_{tet}	pUC19	(3)
pBOMB4-Tet (no GFP)-*MreB*1-69nt-*gfp*	*bla* P_{tet}::*Ctr_mreB*1-69nt-*gfp*	pUC19	This study
pBOMB4-Tet (no GFP)-*MreB*1-84nt-*gfp*	*bla* P_{tet}::*Ctr_mreB*1-84nt-*gfp*	pUC19	This study
pKT25	*aph* P_{lac}::*t25*	p15A	(4)
pUT18C	*bla*P_{lac}::*t18*	ColE1	(4)
pKT25-*mreB*	*aph* P_{lac}::*t25-Ctr_mreB*	p15A	This study
pKT25-*mreB*_67	*aph* P_{lac}::*t25*-ΔN66nt *Ctr_mreB*	p15A	This study
pKT25-*mreB*_85	*aph* P_{lac}::*t25*-ΔN84nt *Ctr_mreB*	p15A	This study
pKT25-*mreB*_97	*aph* P_{lac}::*t25*-ΔN96nt *Ctr_mreB*	p15A	This study
pUT18C-*mreB*	*bla*P_{lac}::*t18-Ctr_mreB*	ColE1	This study

pUT18C-*mreB_67*	*bla*P*lac*::*t18*-ΔN66nt *Ctr_mreB*	ColE1	This study
pUT18C-*mreB_85*	*bla*P*lac*::*t18*-ΔN84nt *Ctr_mreB*	ColE1	This study
pUT18C-*mreB_97*	*bla*P*lac*::*t18*-ΔN96nt *Ctr_mreB*	ColE1	This study
pUT18C-*rodZ*	*bla*P*lac*::*t18-Ctr_rodZ*	ColE1	(5)
pUT18C-*ftsK*	*bla*P*lac*::*t18-Ctr_ftsK*	ColE1	(6)
pUT18C-*ftsK*N	*bla*P*lac*::*t18*-N-terminus of *Ctr_ftsK*	ColE1	(6)
pKT25-zip	*aph* P*lac*::*t25-zip*	p15A	(4)
pUT18C-zip	*bla*P*lac*::*t18-zip*	ColE1	(4)
pTLR2-*mreB-gfp*_sw	*bla* P*tet*::*Ctr_mreB-gfp_sw*	ColE1	This study
pTLR2-*mreB_67-gfp*_sw	*bla* P*tet*::ΔN66nt *Ctr_mreB-gfp_sw*	ColE1	This study
pTLR2-*mreB_85-gfp*_sw	*bla* P*tet*::ΔN84nt *Ctr_mreB-gfp_sw*	ColE1	This study
pTLR2-*mreB_97-gfp*_sw	*bla* P*tet*::ΔN96nt *Ctr_mreB-gfp_sw*	ColE1	This study
pKT25-*Ec_mreB*	*aph* P*lac*::*t25-Ec_mreB*	p15A	This study
pUT18C-*Ec_mreB*	*bla*P*lac*::*t18-Ec_mreB*	ColE1	This study
pTLR2-*mreB_67*_6xH	*bla* P*tet*::ΔN66nt *Ctr_mreB*_6xH	ColE1	This study
pTLR2-*mreB_85*_6xH	*bla* P*tet*::ΔN84nt *Ctr_mreB*_6xH	ColE1	This study
pTLR2-*mreB_97*_6xH	*bla* P*tet*::ΔN96nt *Ctr_mreB*_6xH	ColE1	This study
pFB112	*tet sdiA*	ColE1	(7)
pFB124	*aadA* cI857(Ts) PλR::*mreC mreD*-LE	pSC101	(7)

711

Strain	Relevant genotype	Source of Reference
MG1655	F^-, lambda$^-$, *rph-1*	
FB17	*dadR trpE trpA tna mreBCD<> frt*	(7)
DHT1	F^- *glnV44* (AS) *recA1 endA1 gyrA96* (Nal^R) *thi-1 hsdR17 spoT1 rfbD1 cya-854 ilv-691 ::Tn10 (TetR)*	(8)
P2733	FB17 pFB112 pFB124	(7)

712

Primer name	Sequence	Features	Usage
mreB 5'/pTLR2/LIC_F	tttgtttaactttaagaaggagata ATGAGCCCATACCGCAGC	lower case for plasmid overlap construction	for amplification of *mreB*
mreB6XH/pTLR2/R	ccatttttcacttcacaggtcaacc ttaatggtgatggtgatggtg TACTAAACTCTCTTTTCGTTTCTTCAATTG	lower case for plasmid overlap construction, adds 6xH to *mreB* sequence	for amplification of *mreB*
mreB_1_5'/pBAD 33/F	ttcgagctcggtacccggggatcct tttgtttaactttaagaaggagatataca ATGAGCCCATACCGCAGC	lower case for plasmid overlap construction, adds	for amplification of *mreB*

		Shine-Dalgano (SD) sequence	
mreB_67_5'/pBAD33/F	ttcgagctcggtacccggggatcct tttgtttaactttaagaaggagatatacaatg GGTCGTTTCGATCGTGTATTTAATTTTTTTTC	lower case for plasmid overlap construction, adds Shine-Dalgano (SD) sequence	for amplification of ΔN66nt *mreB*
mreB 3'/pBAD33/LIC_R	ctagaggatccccgggtaccgagct TCATACTAAACTCTCTTTTCGTTTC	lower case for plasmid overlap construction	for amplification of *mreB*s
EcmreB/pBAD33/F	gctcggtacccggggatcct tttgtttaactttaagaaggagatataca ATGTTGAAAAAATTTCGTG	lower case for plasmid overlap construction, adds Shine-Dalgano (SD) sequence	for amplification of *Ec_mreB*
EcmreB/pBAD33/R	caagcttgcatgcctgcagg TTACTCTTCGCTGAACAGG	lower case for plasmid overlap construction	for amplification of *Ec_mreB*
mreB/pBAD33G/F	tgggctagcgaattcgagct tttgtttaactttaagaaggagatataca ATGAGCCCATACCGCAGC	lower case for plasmid overlap construction, adds Shine-Dalgano (SD) sequence	for amplification of *mreB_1-96nt*
mreB1-96nt/pBAD33G/R	gtcgactctagaggatcccc c AAAAAAATTAAATACACGATCGAAACG	lower case for plasmid overlap construction	for amplification of *mreB_1-96nt*
Ctr L2/mreB/pBAD/5'	TATATGGTACCTGATTAACTTTATAAGGAGGAAAAACAT**A**TGAGCCCATACCGCAGCTTATAT	Underline for KpnI site	for amplification of *mreB*_1-69nt and 1-84nt
Ctr L2/mreB_69/pBAD/3'	CGCCCTCTAGA**A**CCCAACGCCTTGTTATACAGACGGTTAGA	Underline for XbaI site	for amplification of *mreB*_1-69nt
Ctr L2/mreB_84/pBAD/3'	CGCCCTCTAGA**T**ACACGATCGAAACGACCCAACGCCTTGTTATAC	Underline for XbaI site	for amplification of *mreB*_1-84nt
mreB_67-84D/pBAD33/F	gctcggtacccggggatcct tttgtttaactttaagaaggagatataca ATGGGTCGTTTCGATCGTG	lower case for plasmid overlap construction, adds Shine-Dalgano (SD) sequence	for amplification of *mreB_67*-84nt-gfp from gBlock
GFP/pBAD33/R	caagcttgcatgcctgcagg TTATTTGTATAGTTCATCCATGCCATG	lower case for plasmid overlap construction	for amplification of *mreB_67*-84nt-gfp from gBlock
Ec mreB/pBAD/5'	CCCCCGAGCTCTGATTAACTTTATAAGGAGGAAAAACAT**A**TGCTGAAAAAATTTCGTGGCATGT	Underline for SacI site	for amplification of Ec_*mreB*

Ec mreB_22/pBAD/5'	CCCCCGAGCTCTGATTAACTTTATAAGGAGGAAAAACATATGTTCTCCAATGACTTGTCCATTGA	Underline for SacI site	for amplification of ΔN21nt Ec_*mreB*
Ec mreB/pBADGFP/3'	ATAATGTCGACCTCTTCGCTGAACAGGTCGCCGCCGTGCATGTCGATC	Underline for SalI site	for amplification of Ec_*mreB*
mreB/pBOMB4/F	gatctaaagaggagaaaggatctgcATGAGCCCATACCGCAG	lower case for plasmid overlap construction	for amplification of *mreB*_1-69nt and 1-84nt fused with *gfp*
GFP/pBOMB4/R	tttgaatggtcgaccggtacTTATTTGTATAGTTCATCCATGCCATG	lower case for plasmid overlap construction	for amplification of *mreB*_1-69nt and 1-84nt fused with *gfp*
mreB_4/T25/F	ctgcagggtcgactctagagAGCCCATACCGCAGCTTATATAAG	lower case for plasmid overlap construction	for amplification of *mreB*
mreB_67/T25/F	ctgcagggtcgactctagagGGTCGTTTCGATCGTGTATTTAATTTTTTTTC	lower case for plasmid overlap construction	for amplification of ΔN66nt *mreB*
mreB_85/T25/F	ctgcagggtcgactctagagTTTAATTTTTTTTCCGGG	lower case for plasmid overlap construction	for amplification of ΔN84nt *mreB*
mreB_97/T25/F	ctgcagggtcgactctagagTCCGGGAATGTTGGTATC	lower case for plasmid overlap construction	for amplification of ΔN96nt *mreB*
mreB_1101/(pKT25)/R	tcacgacgttgtaaaacgacggccgTCATACTAAACTCTCTTTTCGTTTC	lower case for plasmid overlap construction	for amplification of *mreBs*
mreB_4/T18/F	actgcaggtcgactctagagAGCCCATACCGCAGCTTATATAAG	lower case for plasmid overlap construction	for amplification of *mreB*
mreB_67/T18/F	actgcaggtcgactctagagGGTCGTTTCGATCGTGTATTTAATTTTTTTTC	lower case for plasmid overlap construction	for amplification of ΔN66nt *mreB*
mreB_85/T18/F	actgcaggtcgactctagagTTTAATTTTTTTTCCGGG	lower case for plasmid overlap construction	for amplification of ΔN84nt *mreB*
mreB_97/T18/F	actgcaggtcgactctagagTCCGGGAATGTTGGTATC	lower case for plasmid overlap construction	for amplification of ΔN96nt *mreB*
mreB_1101/(pUT	accatattacttagttatatcgatg	lower case for	for

18C)/R	TCATACTAAACTCTCTTTTCGTTTC	plasmid overlap construction	amplification of *mreBs*
Ct009/rodZ/BACTH/5'BamHI	ATATAGGATCCA**G**GTAGAGCAAACCAGGGGAATTAC	Underline for BamHI site	for amplification of *rodZ*
Ct009/rodZ/BACTH/3'KpnI	AGGGTGGTACC**T**TA**G**AAAAGGTTGAATAGATTCCCTAG	Underline for KpnI site	for amplification of *rodZ*
Ct739/ftsK/BACTH/5'XbaI	ACTAGCTGGTTCTAGAT**G**GAAAAGAACGGAAGAAA	Underline for XbaI site	for amplification of *ct739*(*Ctr_ftsK*)
Ct739/ftsK/BACTH/3'KpnI	CACAGCTAGAGGTACCAT**T**TAATCGTCCTGATTTGA	Underline for KpnI site	for amplification of *ct739*(*Ctr_ftsK*)
Ct739/ftsKN/BACTH/5'XbaI	ACTAGTCTAGAT**G**GAAAAGAACGGAAGAAA	Underline for XbaI site	for amplification of N-terminus of *ct739*(*Ctr_ftsK*)
Ct739/ftsKN/BACTH/3'KpnI	CTAGAGGTACCAT**T**TGAGAAATTTTAGGAGA	Underline for KpnI site	for amplification of N-terminus of *ct739*(*Ctr_ftsK*)
mreB67 5'/pTLR2/LIC_F	tttgtttaactttaagaaggagata ATGGGTCGTTTCGATCGTG	lower case for plasmid overlap construction	for amplification of ΔN66nt *mreB*
mreB85 5'/pTLR2/LIC_F	tttgtttaactttaagaaggagata ATGTTTAATTTTTTTCCGGGAATG	lower case for plasmid overlap construction	for amplification of ΔN84nt *mreB*
mreB_97_5'/pTLR2/F	tttgtttaactttaagaaggagata atgTCCGGGAATGTTGGTATC	lower case for plasmid overlap construction	for amplification of ΔN96nt *mreB*
gfp/pTLR2-mreB/LIC F	ttatccgttaggtggaggtagt AGTAAAGGAGAAGCACTTTTC	lower case for plasmid overlap construction	for amplification of *gfp*
gfp/pTLR2-mreB/LIC R	cctgatcactacctcc GAGTCCGGACTTGTATAGTTC	lower case for *mreB* 3' insert DNA overlap construction	for amplification of *gfp*
mreB 5'/pTLR2/LIC_R2	cctttactactacctcc ACCTAACGGATAAGCAGAACCTATAG	lower case for *gfp* insert DNA overlap construction	for amplification of N-terminus of *mreB*

mreB 3'/pTLR2/LIC_F2	caagtccggactc *ggaggtagt* GATCAGGAATTGGAGATG	lower case for *gfp* insert DNA overlap construction, adds link residues, GGS	for amplification of C-terminus of *mreB*
Ec mreB/BACTH/5' Bam	CCTTGGGATCCT**C**TGAAAAAATTTCGTGGCATGT	Underline for BamHI site	for amplification of Ec_*mreB*
Ec mreB/BACTH/3' Sacstp	ATATTGAGCTC**T**TA**C**TCTTCGCTGAACAGGTCGCC	Underline for SacI site	for amplification of Ec_*mreB*
Ec mreB/BACTH/3' Sac	TATATGAGCTCCC**C**TCTTCGCTGAACAGGTCGCC	Underline for SacI site	for amplification of Ec_*mreB*

1. Wickstrum J, Sammons LR, Restivo KN, Hefty PS. 2013. Conditional gene expression in Chlamydia trachomatis using the tet system. PLoS One 8:e76743.
2. Guzman LM, Belin D, Carson MJ, Beckwith J. 1995. Tight regulation, modulation, and high-level expression by vectors containing the arabinose PBAD promoter. J Bacteriol 177:4121-30.
3. Bauler LD, Hackstadt T. 2014. Expression and targeting of secreted proteins from Chlamydia trachomatis. J Bacteriol 196:1325-34.
4. Karimova G, Ullmann A, Ladant D. 2001. Protein-protein interaction between Bacillus stearothermophilus tyrosyl-tRNA synthetase subdomains revealed by a bacterial two-hybrid system. J Mol Microbiol Biotechnol 3:73-82.
5. Ouellette SP, Rueden KJ, Gauliard E, Persons L, de Boer PA, Ladant D. 2014. Analysis of MreB interactors in Chlamydia reveals a RodZ homolog but fails to detect an interaction with MraY. Front Microbiol 5:279.
6. Ouellette SP, Karimova G, Subtil A, Ladant D. 2012. Chlamydia co-opts the rod shape-determining proteins MreB and Pbp2 for cell division. Mol Microbiol 85:164-78.
7. Bendezu FO, de Boer PA. 2008. Conditional lethality, division defects, membrane involution, and endocytosis in mre and mrd shape mutants of Escherichia coli. J Bacteriol 190:1792-811.
8. Dautin N, Karimova G, Ullmann A, Ladant D. 2000. Sensitive genetic screen for protease activity based on a cyclic AMP signaling cascade in Escherichia coli. J Bacteriol 182:7060-6.